

## ***Interactive comment on “Evaluation of the Lattice Boltzmann Method for wind modelling in complex terrain” by Alain Schubiger et al.***

### **Anonymous Referee #1**

Received and published: 19 February 2020

Review of WES-2019-106, “ Evaluation of the lattice Boltzmann method for wind modelling in complex terrain”. by Schubiger et al.

Over all, this manuscript has good quality. The description and presentation of the results are very clear. I have some small comments:

Abstract, Line 5, Please spell out the acronym WAsP .

Abstract, Line 6, LBM is a mesoscopic level method, not microscopic method if one follows the standard definition.

In Introduction section, there are three articles should be cited. One and two are LES for Bolund Hill. The third is using MRT-LBM large eddy simulation for a stable stratified flow over a ridge for a laboratory test case.

C1

Ma, Y., Liu, H. Large-Eddy Simulations of Atmospheric Flows Over Complex Terrain Using the Immersed-Boundary Method in the Weather Research and Forecasting Model. *Boundary-Layer Meteorol* 165, 421–445 (2017). <https://doi.org/10.1007/s10546-017-0283-9>.

DeLeon, R., Sandusky, M. & Senocak, I. Simulations of Turbulent Flow Over Complex Terrain Using an Immersed-Boundary Method. *Boundary-Layer Meteorol* 167, 399–420 (2018). <https://doi.org/10.1007/s10546-018-0336-8>

Wang, Y., MacCall, B.T., Hocut, C.M. Zeng, X., Fernando, H.J.S. Simulation of stratified flows over a ridge using a lattice Boltzmann model. *Environ Fluid Mech* (2018). <https://doi.org/10.1007/s10652-018-9599-3>

Section 2.2, In your regularized-BGK LBM method, do you compute the strain rate tensor for LES using the fluid particle PDF? If so, it is worthwhile to write out the equations for computing the strain rate based on the PDF of the particle because this is critically important.

Section 3.1, In this section, you noted three westerly wind observational cases. It is probably good to point out that only the 270° case was simulated. It is also good to add some description on lateral (North, South) and outflow boundary conditions.

How about the turbulence (such as TKE) comparison? That will substantially improve the paper.

---

Interactive comment on Wind Energ. Sci. Discuss., <https://doi.org/10.5194/wes-2019-106>, 2020.

## ***Interactive comment on “Evaluation of the Lattice Boltzmann Method for wind modelling in complex terrain” by Alain Schubiger et al.***

**Anonymous Referee #2**

Received and published: 13 March 2020

### General comments:

This paper deals with the evaluation of an LBM method for modelling the neutral atmospheric boundary layer over complex terrain. I like the idea to promote LBM for wind energy applications, and found the paper interesting and of overall good quality. Presented results are very encouraging. Although I have some remarks regarding the methodology (see specific comments).

### Specific comments:

The main drawback of this paper lies in the differences between the models that are compared. I understand this is an evaluation of the LBM method, and thus it comes with its own limitations (no terrain fitted meshes in this case). However, there are

C1

large differences in the meshes that are used (fully cartesian versus vertically stretched meshes), but also mesh sizes (quite different cell numbers, probably due to the stretching applied in the NS solver? Why not using some mesh “coarsening” with Palabos?), the turbulence models (LES vs DES), boundary conditions (staircase vs terrain fitted). Under these conditions, it is difficult to compare the models and draw conclusions (thinking about the conclusion regarding the use of roughness boundary conditions in NS solvers). Although it can be understood that solvers are intrinsically different and methodologies adapted to each solver have been used, I think it could have been interesting to reduce the differences when possible, comparing the models using the same meshes (no vertical stretching), similar turbulence models (LES vs LES), and same roughness models (slip and no-slip for the NS solvers).

From my point of view, a first, preliminary study regarding velocity and turbulence intensity profiles on a simple flat terrain could have brought insight to the model comparison, rather than directly addressing the complex terrain case. Even on this complex terrain case, a comparison of the velocity and turbulence intensity profiles (as shown in Bechmann et al.) are missing, and could provide more insight in the comparisons.

I also wonder about the potential of LBM to handle terrain roughness. The authors used wall-slip conditions for the ocean and no-slip conditions on land with the LBM solver. Isn't it possible to account for the terrain roughness more precisely, using partial-slip boundary conditions? Is the use of a logarithmic profile at the inlet sufficient to model an ABL? Some insight would be welcome.

One last point that is missing is the choice of the collision model. A discussion is proposed regarding the different possibilities (SRT, MRT, entropic, etc.), but the choice is made to use the standard BGK model, which is not supposed to be the most stable. Moreover, the choice of the relaxation parameter “tau” is not discussed (i.e. is equation 6 fully respected?). A small discussion on the non-dimensioning procedure could also be interesting.

C2

Finally, the “code and data availability” section is not present. Can the Palabos simulation setup be shared with the community? It would probably help researchers to get more familiar with LBM and its application to wind energy.

- Page 1 Line 13: LBM is said to have a particular ability to automate the geometry. The argument is often retained to promote LBM methods. However, I do not see the advantage of LBM in comparison to cartesian-grid Navier-Stokes solver with immersed boundaries. Can the authors comment on this point?
- Page 5 Line 12: the authors should be more specific regarding the value of the Smagorinsky constant they have used. Also, is it the same Smagorinsky model used in the NS solver?
- Page 6 Line 22: more details should be given regarding the inflow turbulence generation. Is the same methodology used in the NS solver?
- Page 7 Line 8: some details regarding the mesh used for NS simulations are given. From my understanding, the mesh is wall-adapted. The authors should make it clear.
- Page 7 Line 20: average results of the DES simulation should also be shown.
- Page 13 Line 9: I think this conclusion should be argued, and, from my point of view, is not receivable. There are too many differences in the models to draw such a conclusion (different meshes, turbulence models?, different wall boundary conditions, etc.)
- Page 13 Line 13: LBM is said to be 5 times faster than DES. However, the total CPU time is only 30% lower. Perhaps a comment on the mesh size reduction that could be obtained(using mesh refinement techniques) would help clarify the potential of LBM methods to reduce CPU time. Anyway, would it be possible to have similar meshes between LBM and NS even using mesh refinement, and, have LBM solvers the same mesh size requierements than NS solvers?

Technical corrections:

C3

Figures text size should be made uniform in the different plots. In the current version, fontsize is obviously too small to be readable (Figs 1, 4, 5, 6, 7, 8).

Page 1 Line 15 : doubled dots

Page 2 Line 22 : a extremely fine → an extremely fine

Page 4 Eq. 5 : “with” in italic and attached to “ $f_i$ ”

Page 6 Line 40 : “to an total” → “to a total”

Page 9 Line 12: a reference to the figure should be added

Page 11 Line 5: space between “et al.” and parenthesis.

Page 11 Line 6: “summarise” → “summarize”

Page 13 Line 2: “is far” → “it is far” or “LES is far”, or replace “; however” with something else to improve readability

Page 13 Line 8: “of cliff” → “of the cliff”

---

Interactive comment on Wind Energ. Sci. Discuss., <https://doi.org/10.5194/wes-2019-106>, 2020.

C4

## Point-by-point response

### RC1

- Abstract, Line 5, Please spell out the acronym WAsP:

changed in the new version of the paper

- Abstract, Line 6, LBM is a mesoscopic level method, not microscopic method if one follows the standard definition.

changed in the new version of the paper

- In Introduction section, there are three articles should be cited.

added to the new version of the paper

- Section 2.2, In your regularized-BGK LBM method, do you compute the strain rate tensor for LES using the fluid particle PDF?

The implemented regularization process is best described in this work of Jonas Latt and Bastien Chopard. Latt, Jonas, and Bastien Chopard. "Lattice Boltzmann method with regularized pre-collision distribution functions." Mathematics and Computers in Simulation 72.2-6 (2006): 165-168. A reference was added to the new version of the paper.

- Section 3.1, ... It is also good to add some description on lateral (North, South) and outflow boundary conditions.

Description was added to the new version

- How about the turbulence (such as TKE) comparison?

A comparion of the turbulence has been added to the new version of the paper

### RC2

- "quite different cell numbers...":

Exactly, the Fluent mesh was created with the Fluent meshing tool and therefore there were more possibilities to implement local adjustments. It has been added to the paper.

- "Why not use mesh coarsening with Palabos":

Studies that apply the grid refinement capabilities of Palabos were not within the scope of this first study; however, this is will be tested in the future. It has been added to the set-up description.

- "From my point of view.....":

As previous studies have shown that Palabos works well for turbulent flows (Wissocq, Gauthier, et al. "Regularized characteristic boundary conditions for the Lattice-Boltzmann methods at high Reynolds number flows." Journal of Computational Physics 331 (2017): 1-18.), the aim of this study was to specifically test the applicability to wind energy. Bolund Hill was chosen for this due to the quality of available measurement data. It is correct to say that a simpler geometry may have been easier to start with, and we are considering further comparison cases.

- "...turbulence intensity profiles....":

A comparison of the turbulence has been added to the new version of the paper

- "Isn't it possible to account for terrain roughness":

Unfortunately it is not easily possible to account for different surface roughnesses in Palabos at this point. This mentioned on line 11 on page 6. This is a topic that we are planning to investigate in the future.

- "Is the use of a logarithmic profile sufficient?":

We were following the guidelines of the Bolund Hill Blind Test and used the provided logarithmic velocity profile, which were fitted to the measurements.

- "...collision model... The choice of Tau":

The BGK model was chosen for simplicity in this first study. Tau respectively Nu were chosen so we could achieve a stable solution and eq. 6 is respected. This has been described in the new version of the paper

- "A small discussion on the non-dimensioning procedure...":

A reference has been added to the new version.

Latt, Jonas. "Choice of units in lattice Boltzmann simulations." Freely available online at [http://lbmethod.org/\\_media/howtos:lbunits.pdf](http://lbmethod.org/_media/howtos:lbunits.pdf) (2008).

- "Can the Palabos simulation setup be shared with the community":

The code is available on the git repository. The link has been added to the new version of the paper.

- "Page 1 Line 13: LBM is said to have a particular ability...":

It is true. With regard to mesh and geometry generation, the difference to cartesian-grid NS solver with immersed boundaries is not that great, as compared to wall-adapted NS solvers. However, the main advantages LBM like intrinsic massive parallelism or offering simplicity in development are present

- "Page 5, Line 12: Smagorinsky model":

The Smagorinsky constant was set to 0.14. This has been added to the new version of the paper

- "Page 6, Line 22: Is the same methodology used in the NS solver?":

The Fluent setup uses the Synthetic Turbulence Generator scheme. For the LBM simulation we implemented a rudimentary transient inflow condition. The Fluent implementation is much more sophisticated. This is described on page 6 and 7 of the paper".

- "Page 7, Line 20: average results of the DES simulation should also be shown.":

This has been added to the new version of the paper

- "Page 13, Line 9: I think this conclusion should be argued, and, from my point of view, is not receivable.":

Parts of the conclusion have been adjusted and the difference in the simulation approaches have been made clearer. For example the summary: It can be summarised that LBM may be applicable to modelling wind flow over complex terrain accurately at relatively low costs if the challenges raised in this work are addressed. Further studies on other sites are ongoing.

- "Page 13, Line 13: "Perhaps a comment on the mesh size reduction...":

An estimation on the mesh size reduction has been added.

- "would it be possible to have similar meshes between LBM and NS even using mesh refinement, and, have LBM solvers the same mesh size requirements than NS solvers?":

More or less this is possible and is part of a running follow-up project.

- Figure text size and following comments: changed

Page 1 Line 15 : doubled dots

Page 2 Line 22 : a extremely fine → an extremely fine

Page 4 Eq. 5 : "with" in italic and attached to " $f_i$ "

Page 6 Line 40 : "to an total" → "to a total"

Page 9 Line 12: a reference to the figure should be added

Page 11 Line 5: space between "et al." and parenthesis.

Page 11 Line 6: "summarise" → "summarize"

Page 13 Line 2: "is far" → "it is far" or "LES is far", or replace ";" however" with something else to improve readability

Page 13 Line 8: "of cliff" → "of the cliff"

## ***Interactive comment on “Evaluation of the Lattice Boltzmann Method for wind modelling in complex terrain” by Alain Schubiger et al.***

**Alain Schubiger et al.**

alain.schubiger@hsr.ch

Received and published: 16 April 2020

Thank you very much for the comments.

Abstract, Line 5, Please spell out the acronym WAsP: changed in the new version of the paper

Abstract, Line 6, LBM is a mesoscopic level method, not microscopic method if one follows the standard definition. changed in the new version of the paper

In Introduction section, there are three articles should be cited. added to the new version of the paper

Section 2.2, In your regularized-BGK LBM method, do you compute the strain rate

C1

tensor for LES using the fluid particle PDF?

The implemented regularization process is best described in this work of Jonas Latt and Bastien Chopard. Latt, Jonas, and Bastien Chopard. "Lattice Boltzmann method with regularized pre-collision distribution functions." Mathematics and Computers in Simulation 72.2-6 (2006): 165-168. A reference was added to the new version of the paper.

Section 3.1, ... It is also good to add some description on lateral (North, South) and outflow boundary conditions. Description was added to the new version

How about the turbulence (such as TKE) comparison? A comparison of the turbulence has been added to the new version of the paper

---

Interactive comment on Wind Energ. Sci. Discuss., <https://doi.org/10.5194/wes-2019-106>, 2020.

C2

## ***Interactive comment on “Evaluation of the Lattice Boltzmann Method for wind modelling in complex terrain” by Alain Schubiger et al.***

**Alain Schubiger et al.**

alain.schubiger@hsr.ch

Received and published: 16 April 2020

Thank you very much for the comments

- "quite different cell numbers...":

Exactly, the Fluent mesh was created with the Fluent meshing tool and therefore there were more possibilities to implement local adjustments. It has been added to the paper.

- "Why not use mesh coarsening with Palabos":

Studies that apply the grid refinement capabilities of Palabos were not within the scope of this first study; however, this is will be tested in the future. It has been added to the set-up description.

C1

- "From my point of view.....":

As previous studies have shown that Palabos works well for turbulent flows (Wissocq, Gauthier, et al. "Regularized characteristic boundary conditions for the Lattice-Boltzmann methods at high Reynolds number flows." *Journal of Computational Physics* 331 (2017): 1-18.), the aim of this study was to specifically test the applicability to wind energy. Bolund Hill was chosen for this due to the quality of available measurement data. It is correct to say that a simpler geometry may have been easier to start with, and we are considering further comparison cases.

- "...turbulence intensity profiles...":

A comparison of the turbulence has been added to the new version of the paper

- "Isn't it possible to account for terrain roughness":

Unfortunately it is not easily possible to account for different surface roughnesses in Palabos at this point. This mentioned on line 11 on page 6. This is a topic that we are planning to investigate in the future.

- "Is the use of a logarithmic profile sufficient?":

We were following the guidelines of the Bolund Hill Blind Test and used the provided logarithmic velocity profile, which were fitted to the measurements.

- "...collision model... The choice of Tau ":

The BGK model was chosen for simplicity in this first study. Tau respectively Nu were chosen so we could achieve a stable solution and eq. 6 is respected. This has been described in the new version of the paper

- "A small discussion on the non-dimensioning procedure...":

A reference has been added to the new version. Latt, Jonas. "Choice of units in lattice Boltzmann simulations." Freely available online at [http://lbmethod.org/\\_media/howtos](http://lbmethod.org/_media/howtos):

C2

Ibunits.pdf (2008).

- "Can the Palabos simulation setup be shared with the community":

The code is available on the git repository. The link has been added to the new version of the paper.

- "Page 1 Line 13: LBM is said to have a particular ability...":

It is true. With regard to mesh and geometry generation, the difference to cartesian-grid NS solver with immersed boundaries is not that great, as compared to wall-adapted NS solvers. However, the main advantages LBM like intrinsic massive parallelism or offering simplicity in development are present

- "Page 5, Line 12: Smagorinsky model":

The Smagorinsky constant was set to 0.14. This has been added to the new version of the paper

- "Page 6, Line 22: Is the same methodology used in the NS solver?":

The Fluent setup uses the Synthetic Turbulence Generator scheme. For the LBM simulation we implemented a rudimentary transient inflow condition. The Fluent implementation is much more sophisticated. This is described on page 6 and 7 of the paper".

- "Page 7, Line 20: average results of the DES simulation should also be shown.":

This has been added to the new version of the paper

- "Page 13, Line 9: I think this conclusion should be argued, and, from my point of view, is not receivable.":

Parts of the conclusion have been adjusted and the difference in the simulation approaches have been made clearer. For example the summary: It can be summarised that LBM may be applicable to modelling wind flow over complex terrain accurately at relatively low costs if the challenges raised in this work are addressed. Further studies

### C3

on other sites are ongoing.

- "Page 13, Line 13: "Perhaps a comment on the mesh size reduction...":

An estimation on the mesh size reduction has been added.

- "would it be possible to have similar meshes between LBM and NS even using mesh refinement, and, have LBM solvers the same mesh size requirements than NS solvers?":

More or less this is possible and is part of a running follow-up project.

Figure text size and following comments: changed

Page 1 Line 15 : doubled dots

Page 2 Line 22 : a extremely fine -> an extremely fine

Page 4 Eq. 5 : "with" in italic and attached to "f\_i"

Page 6 Line 40 : "to an total" -> "to a total"

Page 9 Line 12: a reference to the figure should be added

Page 11 Line 5: space between "et al." and parenthesis.

Page 11 Line 6: "summarise" -> "summarize"

Page 13 Line 2: "is far" -> "it is far" or "LES is far", or replace ";" however" with something else to improve readability

Page 13 Line 8: "of cliff" -> "of the cliff"

---

Interactive comment on Wind Energ. Sci. Discuss., <https://doi.org/10.5194/wes-2019-106>, 2020.

### C4

# Evaluation of the Lattice Boltzmann Method for wind modelling in complex terrain

Alain Schubiger<sup>1</sup>, Sarah Barber<sup>1</sup>, and Henrik Nordborg<sup>1</sup>

<sup>1</sup>University of Applied Sciences Rapperswil (HSR)

<sup>1</sup>Oberseestrasse 10, 8640 Rapperswil CH

**Correspondence:** A.Schubiger (alain.schubiger@hsr.ch)

**Abstract.** The worldwide expansion of wind energy is making the choice of potential wind farm locations more and more difficult. This results in an increased number of wind farms being located in complex terrain, which is characterised by flow separationand turbulence, turbulence and high shear. Accurate modelling of these flow features is key for the wind resource assessment in the planning phase, as the exact positioning of the wind turbines has a large effect on their energy production and fatigue damagelifetime. Wind modelling for wind resource assessments is usually carried out with the linear model WAsPWind Atlas Analysis and Application Program (WAsP), unless the terrain is highly complex, in which case Reynolds-Averaged Navier-Stokes (RANS) solvers such as WindSim and ANSYS Fluent are usually applied. Recent research has showed shown the potential advantages of Large Eddy Simulations (LES) for modelling the atmospheric boundary layer and thermal effects; however, they are LES is far too computationally expensive to be applied outside the research environment. Another promising approach is the Lattice Boltzmann Method (LBM), a computational fluid technique based on the Boltzmann transport equation. It is generally used to study complex phenomena such as turbulence, because it describes motion at the microscopic mesoscopic level in contrast to the macroscopic level of conventional Computational Fluid Dynamics (CFD) approaches, which solve the Navier-Stokes (N-S) equations. Other advantages of LBM include its efficiency, near ideal scalability on High Performance Computers (HPC) and the capabilities its ability to easily automate the geometry, the mesh generation and the post-processing of the geometry. However, LBM has been applied very little to wind modelling in complex terrain for wind energy applications, mainly due to the lack of availability of easy-to-use tools as well as the lack of experience with this technique. In this studypaper, the capabilities of LBM to model wind flow around complex topography terrain are investigated using the PALABOSPalabos framework and data from a measuring campaign at the Bolund peninsula at the coast of Denmark. The topographic properties of Bolund Hill resemble a typical wind turbine site in complex terrain. Together with the measured data, it represents a good validation case. measurement campaign from the Bolund Hill experiment in Denmark. Detached Eddy Simulations (DES) and LES in ANSYS Fluent are used as a numerical comparison. The first results are promising and the comparison between experimental and simulation data are in good agreement. results show that there is in general a good agreement between simulation and experimental data, and LBM performs better than RANS and DES. Some deviations can be observed near the ground, close to the top of cliff and on the lee side of the hill. The computational costs of the three techniques are compared and it has been shown that LBM can perform up to five times faster than DES, even though the set-up was not optimised in this initial study. It can be summarised that LBM has a very high potential for modelling wind flow over complex

terrain accurately and at relatively low costs, compared to solving the N-S conventionally. Further studies on other sites are ongoing.

## 1 Introduction

30 In order to assess ~~wind resources for the wind resource for both~~ the planning and ~~analysis~~ ~~the assessment~~ of wind farms, measurements and ~~/or simulations of simulations of the~~ prevailing wind conditions are required. Simulations are ~~essential~~, ~~especially for especially crucial in~~ the observation of flows over complex terrain ~~due to the large impact of steep inclines on the flow conditions~~. If the terrain shows only weak topographic changes or low hills, linear models can be used to make fast and sufficiently accurate yield forecasts ~~. The (?)~~. ~~The extremely~~ low computational effort ~~and ease of use~~ makes such models 35 ~~(WASP, WindNinja)~~ the current industry standard. Due to their simplified formulation, however, such models fail in complex terrain and the predictions ~~are unreliable~~ ~~can be unreliable (?)~~. For complex flows, ~~nonlinear~~ ~~non-linear~~ methods that solve the ~~Navier-Stokes (N-S)~~ equations are better suited. The successful use of ~~RANS~~ ~~Reynolds-Averaged Navier-Stokes (RANS)~~ models has been ~~shown in several studies and more and more such methods and tools demonstrated in many studies (e.g. ?, ?, ?, ?)~~ and they are being used ~~in industry (Palm, WindSim)~~. ~~increasingly in the industry. This is reflected by the recent~~ 40 ~~development of wind energy specific tools using RANS-based Computational Fluid Dynamics (CFD), including WAsP-CFD (?) and WindSim (?)~~. The RANS equations govern the transport of the averaged flow quantities, with the whole range of the scales of turbulence being modelled using turbulence closure schemes. The RANS-based modelling approach therefore greatly reduces the required computational effort and resources compared to fully-resolved methods, and is widely adopted for practical engineering applications. A more detailed modelling of turbulence is possible ~~by LES simulations~~ using Large 45 Eddy Simulations (LES). LES lies between Direct Numerical Simulations (DNS) and turbulence closure schemes. The idea of this method is to compute the mean flow and the large vortices exactly. The small-scale structures are not simulated, but their influence on the rest of the flow field is parameterised by a heuristic model. However, the computational effort and the demands on the computational mesh increase drastically ~~over~~ compared to RANS simulations, ~~due to the need to resolve the small and important dynamic eddies in the boundary layer~~. Recent studies of the Bolund Hill blind test also show that it is still 50 a great challenge to achieve sufficiently accurate predictions using LES simulations ~~. The DES (?, ?, ?, ?)~~. This is because, to accurately resolve the small-scale turbulent structures near walls at high Reynolds numbers, an extremely fine grid resolution is required.

The Detached Eddy Simulation (DES) method is a combination of LES and RANS. With this method, the flow is mostly calculated by LES, but the flow and vortices in wall regions are modelled by RANS. ~~However, this~~ ~~This~~ method promises 55 a strong reduction of the computational effort and the mesh requirements ~~compared to LES~~. In addition, boundary layer modelling using RANS models makes it possible to use surface roughness models ~~. An alternative (?)~~.

An alternative to solving the N-S equations with great potential is the ~~LBM~~ Lattice Boltzmann Method (LBM). LBM has become more and more popular in recent years and ~~has been~~ ~~is being~~ continuously developed further. LBM has also been used successfully ~~for initial studies~~ in the field of wind energy. ~~Many~~ ~~Most~~ of these studies focus on the simulation of flows

60 around wind turbines and wind farms or analyse the wake behaviour of turbines (Deiterding, Wood, Asmuth). This studies had e.g. ?, ?). Studies have shown that LBM is a valid alternative to conventional CFD methods and has many advantages (2). The main advantage of the method is its almost ideal scalability. This makes the application on high performance computers High Performance Computers (HPC) attractive, but GPU-based Graphics Processing Unit (GPU) -based LBM codes have also been implemented recently (?, ?). This makes it possible to perform computationally intensive LES simulations on a simple 65 workstation/desktop in a reasonable time (Asmuth)(?). However, LBM has not been used very much yet been assessed a great deal for the calculation of wind fields in complex terrain -for wind energy applications.

The goal of this study is present paper is therefore to evaluate the capabilities of LBM for the applications in wind simulations. Ansys wind modelling in complex terrain. ANSYS Fluent is used as reference general flow solver. With Fluent we also discuss two turbulence modelling approaches, RANS and DES. RANS simulations are cheaper regarding computational 70 cost but do not depict the instantaneous flow and turbulence characteristics as detailed as LES or DES simulations are capable for comparisons, using both a RANS and a DES approach. The paper starts with a brief introduction of the theories behind LBM and the conventional Navie-Stokes based N-S-based CFD calculations in Section ??, and the methods to calculate turbulence, then introduces the simulation method applied in Section ??, discusses the results in Section ??, and finishes with the conclusions in Section 5.

## 75 2 Lattice Boltzmann framework for isothermal flow Method theory

### 2.1 Numerical method and governing equations

The interest in LBM has been growing in the past decades as an efficient method for computing various fluid flows, ranging from low-Reynolds-number flows to highly turbulent flows (e.g. ?, ?). The first LBM models struggled with high-Reynolds-number flows due to numerical instabilities. To solve this problem various adaptions like regularized, various adaptions 80 such as regularised Finite Difference (?), multiple relaxation time (MRT) (?) or entropic methods (?) were have been developed.

LBM is seen to be superior to has the following advantages over N-S equation based solvers due to the following reasons. 1. LBM can present rich and complex physics. A linear equation with only local instability, making it more stable and perfectly scalable, 2. Turbulent and thermal fluctuations are coupled at the same level. The dissipation is introduced locally by the collision term and does not depend on the lattice, and 3. The relaxation time - the relaxation time includes both the regular 85 viscous effects and its higher order modifications (?). A description of LBM can be found, for example in ?. The governing equations describe the evolution of the probability density of finding a set of particles with a given microscopic velocity at a given location:

$$f_i(\mathbf{x} + \mathbf{c}_i \Delta t, t + \Delta t) = f_i(\mathbf{x}, t) + \Omega_i(\mathbf{x}, t) \quad (1)$$

for  $0 \leq i \leq q$ , where  $c_i$  represents a discrete set of  $q$  velocities,  $f_i(\mathbf{x}, t)$  is the discrete single particle distribution function corresponding to  $c_i$  and  $\Omega_i$  an operator representing the internal collisions of pairs of particles. Macroscopic values such as density  $\rho$  and the flow velocity  $\mathbf{u}$  can be deduced from the set of probability density functions  $f_i(\mathbf{x}, t)$ , such as:

$$\rho = \sum_{i=0}^{q-1} f_i, \quad \rho \mathbf{u} = \sum_{i=0}^{q-1} f_i c_i \quad (2)$$

The set of allowed velocities in LBM is restricted by conservation of mass and momentum and by rotational symmetry (isotropy). Some of the most popular choices for the set of velocities are D2Q9 and D3Q27 lattices, respectively 9 referring to nine velocities in 2D and 27 velocities in 3D. For both of these lattices, the sound speed speed of sound in lattice units is given by  $c_s = 1/\sqrt{3}$  (?). The collision operator  $\Omega_i$  is typically modelled with the Bhatnagar–Gross–Krook (BGK) approximation (?), which consists in a relaxation, with a. It assumes that the fluid locally relaxes to equilibrium over a characteristic, non-dimensional timescale  $\tau$ . The relaxation time  $\tau$  of every population to the determines how fast the fluid approaches equilibrium and is thus directly dependent on the viscosity of the fluid. The corresponding equilibrium probability density function  $f_i^{(eq)}$  is defined as:

$$\Omega_i = -\frac{1}{\tau} \left[ f_i(\mathbf{x}, t) - f_i^{(eq)}(\mathbf{x}, t) \right] \quad (3)$$

The equilibrium distribution function  $f_i^{(eq)}$  is a local function that only depends on density and velocity in the isothermal case. It can be computed thanks to a second order development of the Maxwell–Boltzmann equilibrium function (?):

$$f_i^{(eq)} = w_i \rho \left[ 1 + \frac{\mathbf{c}_i \cdot \mathbf{u}}{c_s^2} + \left( \frac{\mathbf{c}_i \cdot \mathbf{u}}{2c_s^2} \right)^2 - \frac{\mathbf{u}^2}{2c_s^2} \right] \quad (4)$$

where  $w_i$  refers to the gaussian weights of the lattice. A Chapman–Enskog expansion, based on the assumption that  $f_i$  is given by the sum of the equilibrium distribution plus a small perturbation  $f_i^1$ :

$$f_i = f_i^{(eq)} + f_i^1, \quad \text{with, with } f_i^1 \ll f_i^{(eq)} \quad (5)$$

can be applied to equation ?? in order to recover the exact N-S equation for quasi-incompressible flows in the limit of long-wavelength (?). The lattice pressure is thus given by  $p = c_s^2 \rho$  the kinematic and the lattice viscosity is linked to the BGK relaxation parameter through:

$$\nu = c_s^2 \left( \tau - \frac{1}{2} \right) \quad (6)$$

The Chapman–Enskog expansion also relates the second order tensor  $\Pi^{(1)}$  defined as:

$$\Pi^{(1)} = \sum_i \mathbf{c}_i \mathbf{c}_i f_i^{(1)}$$

115 with the strain rate tensor  $\mathbf{S} = (\nabla \mathbf{u} + (\nabla \mathbf{u})^T)/2$  through the relation

$$\underline{\Pi^{(1)} = -2c_s^2 \rho \tau \mathbf{S}}.$$

In turn to the leading order  $f_i^{(1)}$  can be approximated by

$$\underline{f_i^{(1)} \cong \frac{w_i}{2c_s^2} \mathbf{Q}_i : \Pi^{(1)}},$$

where  $\mathbf{Q}_i = (\mathbf{e}_i \mathbf{e}_i - c_s^2 \mathbf{I})$ . The colon symbol stands for the double contraction operator and  $\mathbf{I}$  is the identity matrix.

120 The numerical scheme is divided in two steps:

- A collision step where the BGK model is applied:

$$f_i(\underline{\left(\mathbf{x}, t + \frac{1}{2}\right)}) = f_i(\mathbf{x}, t) + \frac{1}{\tau} \left[ f_i^{(eq)}(\mathbf{x}, t) - f_i(\mathbf{x}, t) \right] \quad (7)$$

- A streaming step:

$$f_i(\underline{\mathbf{x} + \mathbf{c}_i, t + 1}) = f_i(\underline{\left(\mathbf{x}, t + \frac{1}{2}\right)}). \quad (8)$$

125 In the collision step particle populations interact and change their velocity directions according to scattering rules. This operation is completely local which makes LBM well suited for parallelism. The streaming step consists in of an advection of each discrete population to the neighbor neighbour node located in the direction of the corresponding discrete velocity. Since a boundary node has less neighbors neighbours than an internal node (less than 9 neighbors in 2D or 27 neighbors in 3D), some populations are missing at the boundary after each iteration. These populations need to be reconstructed, which is the 130 purpose of the implementation of boundary conditions in LBM.

## 2.2 Turbulence modelling

Turbulence causes leads to the appearance of eddies with a wide range of length and time scales which interact, which interact with each other in a dynamically complex way. Given the importance of the avoidance or promotion of turbulence in engineering applications, it is no surprise that a substantial amount of research effort is dedicated to the development of numerical 135 methods to capture the important effects due to turbulence. The methods can be grouped into the following four categories:

- Turbulence models for Reynolds-averaged Reynolds-Averaged Navier–Stokes (RANS) equations
- Large eddy simulation Eddy Simulation (LES)
- Detached eddy simulation Eddy Simulation (DES)
- Direct numerical simulation Numerical Simulation (DNS)

140 In this work RANS and DES are used for the Fluent simulations and LES. LES was applied for the LBM simulation. simulations. LES is an intermediate form of turbulence calculations which calculates calculation which simulates the behaviour of the larger eddies. The method involves spacial filtering, which passes the larger eddies and rejects the smaller eddies. The effects on the resolved flow (mean flow plus large eddies) due to the smallest, unresolved eddies are included by means of a so-called sub-grid scale model. It is assumed that the subgrid sub-grid scales have the effect of a viscosity correction, which 145 is proportional to the norm of the strain-rate tensor at the level of the filtered scales,  $\nu = \nu_0 + \nu_T$ .  $\nu_T$  is defined as

⋮

$$\nu_T = (C\Delta)^2 |S| \quad (9)$$

where  $C$  is the Smagorinsky constant,  $\Delta$  is the grid size and the tensor-norm of the strain rate is defined as  $|S| = \sqrt{S : S}$ . The value of the Smagorinsky constant depends on the physics of the problem and usually varies between 0.1 150 and 0.2 far from boundaries (??).

### 3 Simulations

#### 3.1 The Bolund Hill Experiment

The Bolund field campaign took place from December 2008 to February 2009 on the Bolund Hill in Denmark. Bolund Hill is a 130 m long (east–west axis), 75 m wide (north–south axis) and 11.7 m high hill, situated near the Risø Campus 155 of the Technical University of Denmark. Details of the experiment are described in ?. The campaign showed dominant wind directions from the west and south-west. Thus the wind has an extensive upwind fetch over the sea before encountering land, leading to a “steady” flow on the windward side of the hill. The wind first encounters a 10-m 10 m vertical cliff, after which air flows back down to sea level on the east side of the hill. A recirculation zone and a flow separation are expected due to this abrupt change of slope. During the campaign, 35 anemometers were deployed over the hill. The location of the measurement 160 devices can be seen on Figure ???. Instrumentation includes included 23 sonic anemometers, 12 cup anemometers and two lidars. At each measurement location, the three components of the wind velocity vector and their variances were recorded for four different dominant wind directions, three westerly winds originating from the sea (268°, 254° and 242°) 268°, 254° and 242° and one easterly wind originating from the land (95°). The mean wind speed during the measurements was around  $10 \text{ ms}^{-1}$ , leading to a Reynolds number of  $Re = Uh/\nu$   $Re = uh/\nu \approx 10^7$  (??) with the free stream velocity  $u = 10 \text{ ms}^{-1}$ , the hill height 165  $h$  and the kinematic viscosity  $\nu$ . The measured values are 10-min ten minute averages of measurements sampled at 20 Hz for sonic anemometers. We followed ? and considered the atmosphere as neutral.

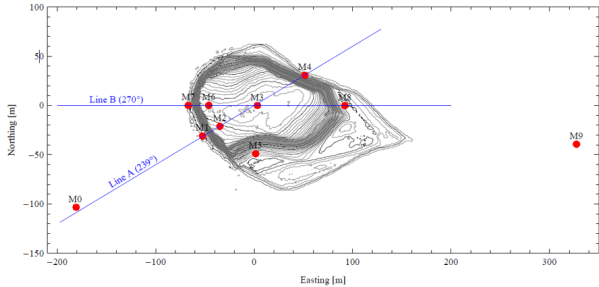


**Figure 1.** A contour map of Bolund [Hill](#) with meteorological masts denoted from M0 to M9. A value of 0.75m has been used for the water level.

### 3.2 [Simulation Set-Up](#)

#### 3.2 [Boundary Condition](#)

$$u(z_{agl}) = \frac{u_* 0}{\kappa} \ln\left(\frac{z_{agl}}{z_0}\right)$$

170 3.2 [Palabos](#) [Simulations Set-Up](#)

##### 3.2.1 [Boundary Conditions](#)

###### [Palabos](#)

The LBM flow solver used in this work ~~is~~ [was](#) the Palabos open-source library [\(2\)](#). The Palabos library is a framework for general-purpose CFD with a kernel based on ~~the~~ LBM. The use of C++ code makes it easy [for experienced programmers](#) to 175 install and [to run on every](#) run on any machine. It is thus possible [for experienced modellers](#) to set up fluid flow simulations with relative ease and to extend the open-source library with new methods and models, which is of paramount importance for the implementation of new boundary conditions.

To calculate the wind fields with Palabos [in this work](#) a 525 m long (east-west axis), 250 m wide (north-south axis) and 40 m high domain with a [uniform](#) grid resolution of  $\Delta x = \Delta y = \Delta z = 0.5\text{m}$  [was used. Leading to an](#)  $\Delta x = \Delta y = \Delta z = 0.5\text{ m}$  [was used, leading to a](#) total cell count of 46 million. [Palabos has the capability to include multiple grid sizes \(octree grid structure\)](#) [to refine the grid near the hill and coarsen it in the far-field, however these techniques were not in the scope of this first study.](#)

There are no [roughness wall models implemented yet. Therefore](#) turbulence closure models or surface roughness models [implemented in the Palabos library yet, therefore](#) the water surfaces were prescribed as free-slip bounce back nodes and the ground [surface surfaces](#) were modelled using [Regularized Regularised](#) Bounce Back nodes [\(?, ?\)](#). The [bounce-back scheme](#) [in this first study was chosen due to its simple implementation and robustness. There are more sophisticated models, like](#)

the Immersed Boundary Method, which may provide better accuracy than the staircase approximation of bounce-back nodes, which will be investigated in further studies.

The inlet profile was described according to the measured wind speeds. Additionally Bolund Hill Blind test specification for the westerly wind case. The logarithmic velocity profile is defined as:

$$190 \quad u(z_{agl}) = \frac{u_{*0}}{\kappa} \ln \left( \frac{z_{agl}}{z_0} \right) \quad (10)$$

with  $\kappa = 0.4$ , the friction velocity  $u_{*0} = 0.4$ , the elevation above ground level  $z_{agl} = z - gl$  ( $gl = 0.75$  m) and the roughness length  $z_0 = 0.0003$  m. Additionally, a time varying fluctuation of the wind speed, corresponding to the given turbulence intensity value, was implemented superposed. The logarithmic wind profile was updated every second during the simulation.

$\Delta t = 0.00289017$  The Atmospheric Boundary Layer (ABL) was considered neutral and thermal effects are therefore neglected.

195 Both sides and top of the domain were modelled as free-slip walls (zero normal velocity). The outlet was set to a constant pressure. Each simulation was run for 600 s with a time step  $\Delta t = 2.89$  ms, leading to around 10 advection times. The relaxation time  $\tau$ , respectively the viscosity  $\nu$ , was chosen to respect eq. ?? and to stabilise the solution. The Smagorinsky constant was set to 0.14.

### 3.3 Fluent

#### 200 Fluent

ANSYS Fluent contains the broad, physical modeling modelling capabilities needed to model flow, turbulence, heat transfer and reactions for industrial applications, ranging from air flow over an aircraft wing to combustion in a furnace, from bubble columns to oil platforms, from blood flow to semiconductor manufacturing and from clean room design to wastewater treatment plants. In this paper, Fluent was first set up to solve the Reynolds-Averaged Navier-Stokes (RANS) equations. The RANS

205 equations govern the transport of the averaged flow quantities, with the whole range of the scales of turbulence being modeled. The RANS-based modeling approach therefore greatly reduces the required computational effort and resources, and is widely adopted for practical engineering applications. The k-epsilon turbulence model was applied to attain closure. This differs from the Large Eddy Simulation (LES) approach, which explicitly computes large eddies in a time-dependent simulation using the 'filtered' N-S equations. The rationale behind LES is that by modeling less of turbulence (and resolving more), the error 210 introduced by turbulence modeling can be reduced. It is also believed to be easier to find a "universal" model for the small scales, since they tend to be more isotropic and less affected by the macroscopic features like boundary conditions, than the large eddies. Filtering is essentially a mathematical manipulation of the exact N-S equations to remove the eddies that are smaller than the size of the filter, which is usually taken as the mesh size. Like Reynolds-averaging, the filtering process creates additional unknown terms that must be modeled to achieve closure. Statistics of the time-varying flow fields such as 215 time-averages and r.m.s. values of the solution variables, which are generally of most engineering interest, can be collected during the time-dependent simulation.

For the Fluent simulation the For the Fluent simulations in this work the mesh was created with the new improved Fluent meshing tool, additionally the domain was extended to 830 m x 450 m x 60 m and two mesh refinement zones near the hill were implemented. The mesh resolution ranged from 0.5 m near the hill up to 15 m in the far-field, resulting in a total cell count 220 of 10 million. A roughness length of  $z_0 = 0.3\text{ mm}$  was prescribed for the water surface and a roughness length of  $z_0 = 15\text{ mm}$  for the ground surfaces.  $\Delta t = 0.05$  The RANS simulation, using the  $k-\omega$  SST turbulence model, was used to initialise the flow and turbulence quantities for the DES simulation. Each simulation was run for 600 s. ~~Leading to around 10 advections with a time step  $\Delta t$  of 50 ms, leading to around seven advection times for the Palabos simulation and around 7 for the DES Fluent simulations. Fluent: -log profile experiment -RANS TI-DES vortex generator~~

225 ~~Boundary Condition Palabos LES Fluent RANS Fluent DES Inlet Turbulence generation Time varying  $\propto$  TI TI~~ The inlet velocity was described as discussed before. According to the Blind Test, the turbulent kinetic energy (TKE) at the inlet was set to  $0.928\text{ m}^2\text{s}^{-2}$ . For the DES model the Synthetic Turbulence Generator ~~ABL stability Outlet Lateral Surface Roughness model~~ ~~Domain size 525 m x 250 m x 40 m 830 m x 450 m x 60 m 830 m x 450 m x 60 m~~ scheme was used to generate a time-dependent inlet condition. It uses a Fourier based synthetic turbulence generator. This method is inexpensive in terms 230 of computational time compared with the other existing methods while achieving high quality turbulence fluctuations (?). Free-slip boundary condition is used for all the flow variables at the top and the side boundaries. The Smagorinsky constant was set to 0.14.

## 4 Results and Discussion

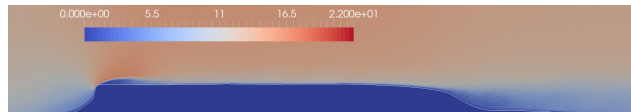
In this section we use the same methodology used

235 **4.1 Flow comparisons**

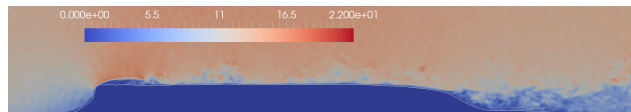
The calculated velocity magnitude fields at a vertical plane through the position of met mast M3 for each measurement technique are shown in Fig. ?? and Fig. ?? . The LBM results are shown in Fig. ??, in terms of the averaged velocity magnitude over the simulation time (a) and the instantaneous velocity magnitude at time  $t = 600\text{ s}$  (b). Fig. ?? and ?? show the averaged 240 velocity magnitude over the simulation time for the RANS and DES simulations and Fig. ?? shows the instantaneous velocity magnitude at time  $t = 600\text{ s}$  for DES. It is interesting to note the separation region as the wind flows over the sharp edge of the hill, as well as the highly separated flow at its rear side.

### 4.2 Performance comparisons

For a quantitative comparison, the same methodology is used as described by ? for the wind flow along the  $270^\circ$  axis (??) . We compare and quantify  $270^\circ$  axis (Case 1) as shown in Fig. ?? . This involved investigating the difference between measurements



(a) Averaged velocity field.



(b) Instantaneous velocity field at  $t = 600$  s (LBM).

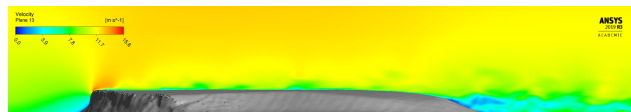
**Figure 2.** Velocity field over the hill along the B line (LBM)



(a) Averaged velocity field (RANS).



(b) Averaged velocity field (DES).



(c) Instantaneous velocity field (DES).

**Figure 3.** Velocity field over the hill along the B line (Fluent results)

245 and simulations after the mast M0 by comparing and quantifying the changes in the wind field as either both changes in speed (so-called "speed-up") or ("and) in direction (turning so-called "turning"). Speed-up is defined by as:

$$\Delta S_m = \frac{\langle \bar{s}/u_{*0} \rangle_{z_{agl}} - \langle \bar{s}_0/u_{*0} \rangle_{z_{agl}}}{\langle \bar{s}_0/u_{*0} \rangle_{z_{agl}}} \frac{\langle \bar{s} \rangle_{z_{agl}} - \langle \bar{s}_0 \rangle_{z_{agl}}}{\langle \bar{s}_0 \rangle_{z_{agl}}} \quad (11)$$

where  $\bar{s}$  is the mean wind speed at the sensor location and  $\bar{s}_0$  is the mean wind speed at the inflow mast M0. Turning is defined as the difference between the wind direction at the measurement point and that at M0. Speed-up along the Bolund Hill. 250 Wind direction is from  $270^\circ$ . Turning along the Bolund Hill. Wind direction is from  $270^\circ$ . Instantaneous velocity field over the hill along the B-line. Averaged velocity field over the hill along the B-line.

The comparison is made in Fig. ?? for two different elevations, 2 m and 5 m above the ground level and for the four mast along the B-line masts along the B line (M7, M6, M3 and M8). The simulation results for the speed-up (??) Fig. ?? show

good agreement with experimental data for all simulation techniques at 5 m above ground level. The (agl), with all deviations

255 lower than 7.1% and the average speed-up error for each simulation technique shown in Table ???. The average speed-up error is defined as:

$$R_s = 100(\Delta S_s - \Delta S_m) \quad (12)$$

where  $S_m$  is the measured speed-up and  $S_s$  is the simulated speed-up defined by Eq. ???. Table ?? also allows the three simulation techniques to be compared to each other. The results 2 m above ground level show some deviations at M2. Overall

260 all the simulation techniques used show slightly higher speed-ups at mast M2. This agl show higher deviations in general, with the average speed-up error for each simulation technique shown in Table ???. The highest discrepancy can be seen at M6, which is probably due to the separation bubble observed in the velocity fields in Fig. ???. The experiment showed reduction in wind speed at M6, whereas the simulations all show an increase in wind speed. This leads to the conclusion that the actual separation bubble is larger than the simulated one. This could be due to an error in the CAD capture of the overhang of the 265 hill noted in previous studies (?). Furthermore, all the simulation techniques under-predicted the negative speed-up in the highly separated region of M8 compared to the experiment. The reason for this is probably due to the well-known difficulty of correctly simulating the separation point in CFD. As this effect is particularly pronounced at a height of 2 m above ground, it may be due to the fact that the lower measuring points lie within the boundary layer. The mast M2 in particular is located 270 directly behind the detachment edge, and the used models were not able to capture the near-wall flow entirely correctly, perhaps due to the assumptions regarding surface roughness.

As shown in Table ??, the most accurate overall prediction was the LBM simulation, with an average error over all the measurement positions of 8.0%. The RANS and DES mean errors are 10.0% and 17.3%, respectively. All three methods showed significantly more accurate results at 5 m than at 2 m above ground.

For the turning of the wind(??) we can see a similar behaviour can be observed. The results match the experimental data 275 very good well at 5 m above ground level but deviate more agl, with all deviations lower than 3.0% and the average turning error for each simulation technique shown in Table ???. As for the speed-up, the deviations in turning are higher at 2 m agl. The most deviation can be noticed, with the average turning error for each simulation technique shown in Table ???. The highest discrepancy can be seen at M8. Met mast M8 is located at the leeside lee side in the recirculation zone of the hill and all. All the simulation results struggle to capture the flow correctly. 280 accurately in terms of the turning. This could be due to the inaccuracy in predicting the exact separation location on the rear of the hill, as mentioned above.

Further analysis using the entire set of measurement data is shown in Fig. ??, in which a comparison between the simulation and experimental data for all three simulation methods is shown. Overall there is a good agreement between the measurements and simulated results. M2 and M6, both right after the edge of the cliff, show the biggest mismatch due to the detached flow 285 after the edge of the hill, as discussed above. The next two figures show the ratio of simulated wind speeds to measured wind speeds as function of elevation (Fig. ??) and measurement location (Fig. ??). The biggest deviation between the data can again be seen at lower heights and at mast M2, M6 and M8. Between the simulation methods, LBM shows the highest averaged

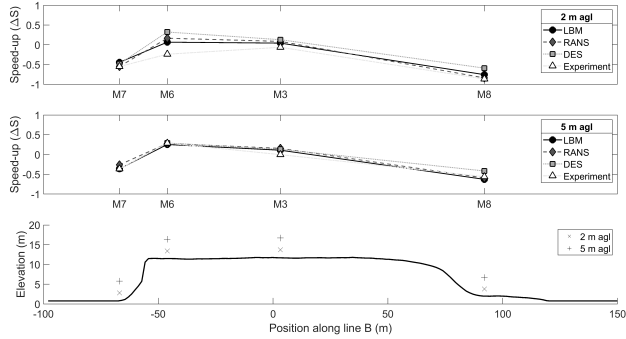


Figure 4. Speed-up along the Bolund Hill. Wind direction is from  $270^\circ$

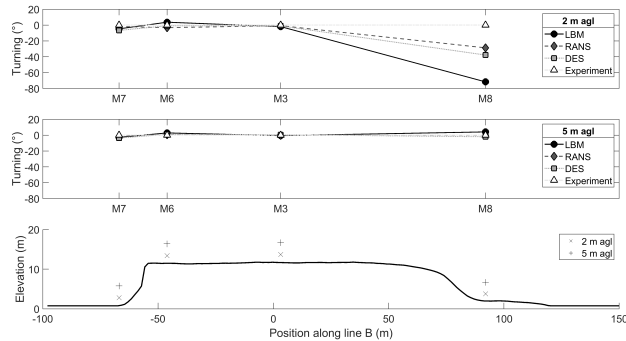


Figure 5. Turning along the Bolund Hill. Wind direction is from  $270^\circ$

deviation of the ratios. The DES and RANS model perform both better in this comparison. This may be due to both these models use the  $k-\omega$  SST turbulence model and incorporate the surface roughness to calculate the near wall turbulence. The 290 reason for the DES model performing worse than the RANS model is unclear at this point and requires further investigation.

Finally figure ?? shows the simulated turbulence kinetic energy (TKE) compared to the measurements for met masts M7, M6, M3 and M8. Overall there is not a particularly good agreement between the measured and simulated data. All the simulations show similar but lower values for TKE. Especially at M6, at the cliff, the deviation is the highest. This discrepancy is being further investigated, but several authors have reported difficulties in simulating a horizontally homogeneous ABL flow in at 295 least the upstream part of computational domains (?, ?).

### 4.3 Cost comparisons

In this section, the performance of the simulation techniques is compared in terms of the computational costs. This has been done because the overall cost of a simulation is an important factor for modellers, who need to choose the most suitable model 300 for a given wind energy project. The results of this work have been used in order to develop a new method for helping wind

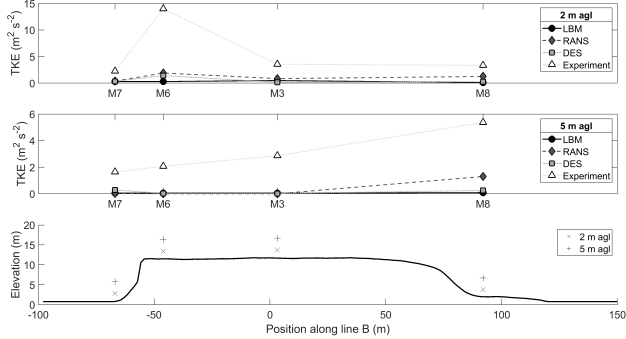


**Figure 6.** Turbulence kinetic energy along the Bolund Hill. Wind direction is from 270°

**Table 1.** Average Speed-up error

	Error at 2 m	Error at 5 m	Average error
Palabos LES	15.7	0.3	8.0
Fluent RANS	14.6	5.5	10.0
Fluent DES	27.4	7.1	17.3

modellers choose the most cost-effective model for a given project. This was done by firstly defining various parameters for predicting the skill and cost scores before carrying out the simulations as well as for calculating skill and cost scores after carrying out the simulations. Weightings were then defined for these parameters, and values assigned to them for a range of tools, including the ones applied in the present work, using a template containing pre-defined limits in a blind test. This allowed 305 a graph of predicted skill score against cost score to be produced, enabling modellers to choose the most cost-effective model without having to carry out the simulations beforehand. More details can be found in ?.

Figure ?? and Table ?? summarise the computational costs for the three different techniques applied in this paper. It can clearly be seen that the LBM performed five times faster than the DES simulation and only slightly slower than the steady 310 RANS simulation. This is due to its explicit formulation and exact advection operator. Furthermore, each of the collision and streaming processes are independent at each lattice, which makes the method so suitable for parallelisation. This advantage extends also to other types of high performance hardware like Graphics Processing Units (GPUs). Some studies of GPUs-based LBM solvers show promising results in this field (? , ? , ?). The performance of this LBM simulation could be increased by adapting the code to use different grid sizes, depending on the flow and therefore reducing the overall cell count drastically. Incorporating the same grid refinement zones as used in the Fluent simulation, while maintaining the extended domain zone, 315 the cell count for the resulting grid would decrease by a factor of five to seven. Work on this is ongoing.

**Table 2.** Average Turning error

	Error at 2 m	Error at 5 m	Average error
Palabos LES	-6.2	0.9	-2.7
Fluent RANS	3.0	0.4	0.2
Fluent DES	-2.7	1.7	-2.0

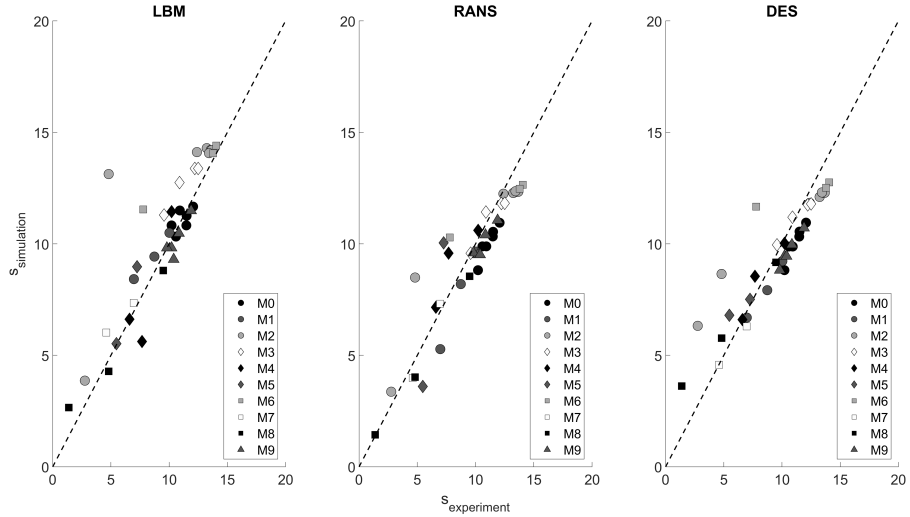


**Figure 7.** Scatter plot of wind speeds, measurement against simulation results

## 5 Conclusion

In this study, a LES simulation using the LBM framework Palabos was implemented to calculate the wind field over the complex terrain of the Bolund Hill. Advantages of LBM include its efficiency, near ideal scalability on High Performance Computers (HPC) and the capabilities to easily automate the geometry, the mesh generation and the post-processing.

320 **TEXT** The results were compared to RANS and DES simulations using ANSYS Fluent and field measurements. In general there was a good agreement between simulation and experimental data. The average wind speed-up error compared to measurements was 8.0% for LBM, 17.3% for DES and 10.0% for RANS. The average wind turning error compared to measurements was 2.7° for LBM, 2.0° for DES and 0.2° for RANS. Some deviations could be observed near the ground, close to the top of the cliff (M2) and on the lee side of the hill (M8). Larger deviations could be observed for the TKE calculation, especially at met 325 mast M6, which is positioned right after the edge of the cliff. This corresponds to previous work, which shows difficulties in correctly resolving the TKE.

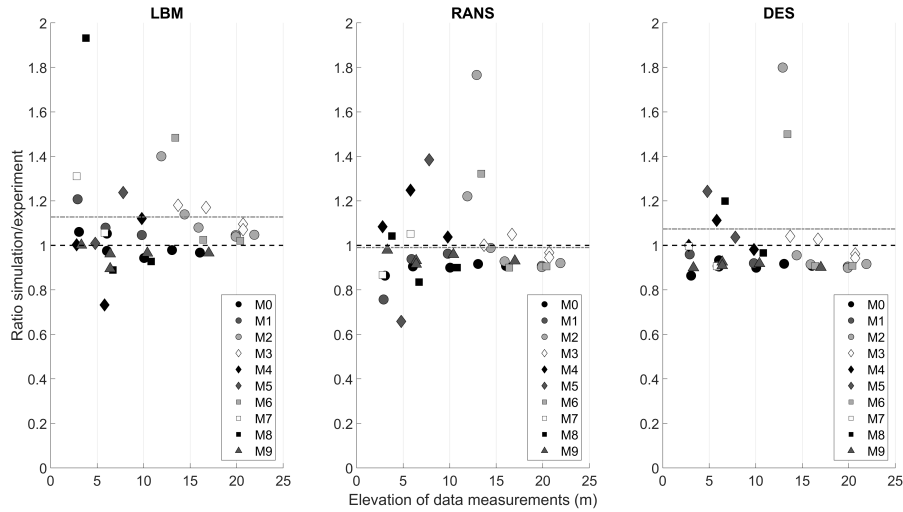


**Figure 8.** Ratio of simulation results to experimental wind speeds as function of elevation. The dotted grey line represents the average value.

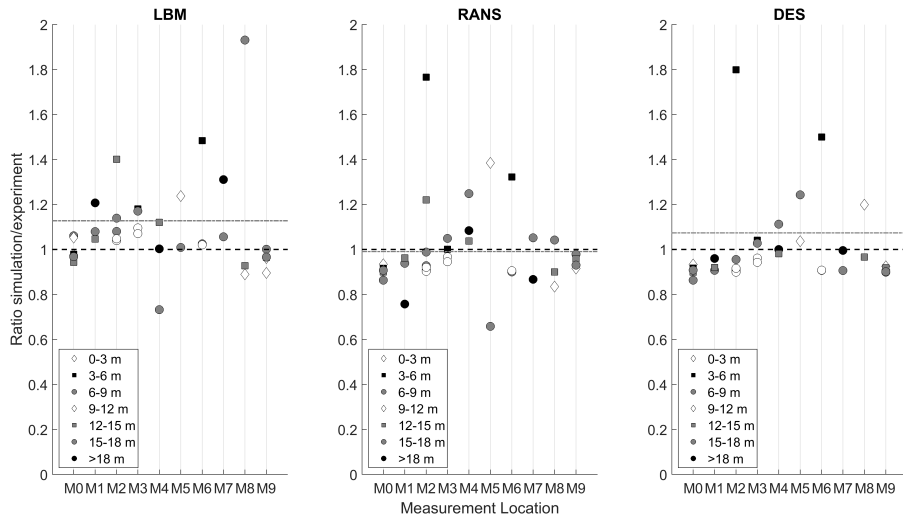


**Figure 9.** Ratio of simulation results to experimental wind speeds as function of measurement location. The dotted grey line represents the average value.

The computational costs of these three models were compared and it has been shown that LBM, even in this not-yet fully optimised set-up of the simulation, can perform five times faster than DES and lead to slightly more accurate results.

It can be summarised that LBM may be applicable to modelling wind flow over complex terrain accurately at relatively low costs if the challenges raised in this work are addressed. Further studies on other sites are ongoing.

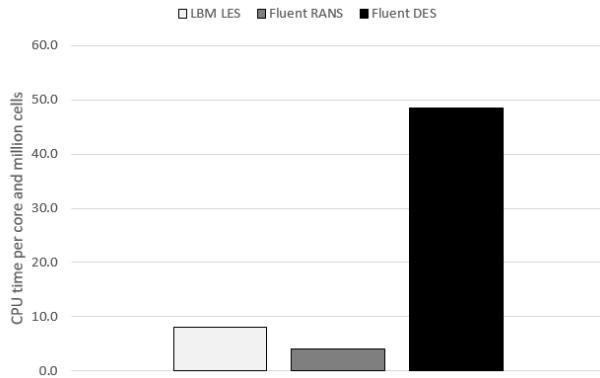


**Figure 10.** Comparison of computational time per cpu core and million cells

*Code availability.* [https://gitlab.com/aschubig/lbm\\_bollundhill.git](https://gitlab.com/aschubig/lbm_bollundhill.git)

#### Appendix A: ConclusionNon-dimensioning procedure

The non-dimensioning procedure used in this study is done according to the similarity theory. It consists of two steps. First a physical system is converted into a dimensionless, independent of the original physical scales, but also independent of simulation parameters. In a second step, the dimensionless system is converted into a discrete simulation. Thus the dimensionless level (D) links the physical system (P) with the discrete Lattice-Boltzmann system (LB). The solutions to the incompressible Navier-Stokes equations for example depend only on the Reynolds number (Re). Thus, the three systems are defined to have the same Reynolds number. The transition from (P) to (D) is made through the choice of a characteristic length scale  $l_0$  and time scale  $t_0$ , and the transition from (D) to (LB) through the choice of a discrete space step  $\Delta x$  and time step  $\Delta t$  (?).

335

340 **A1**

*Author contributions.* The contribution of the authors in this paper is:

- Alain Schubiger: carrying out and analysing the simulations.
- Sarah Barber: project management and paper correction.
- Henrik Nordborg: supervision of Alain Schubiger and paper correction.

345 **TEXT**

## References

Ansumali, S. and Karlin, I. V.: Stabilization of the lattice Boltzmann method by the H theorem: A numerical test, *Physical Review E*, 62, 7999, 2000.

350 **ANSYS: Fluent Theory Guide**, 2019.

Asmuth, H., Olivares-Espinoza, H., Nilsson, K., and Ivanell, S.: The Actuator Line Model in Lattice Boltzmann Frameworks: Numerical Sensitivity and Computational Performance, in: *Journal of Physics: Conference Series*, vol. 1256, p. 012022, IOP Publishing, 2019.

Barber, S.: Comparison metrics microscale simulation challenge for wind resource assessment – stage 1, <https://doi.org/10.5281/zenodo.3743247>, <https://doi.org/10.5281/zenodo.3743247>, 2020.

355 Bechmann, A.: WAsP CFD A new beginning in wind resource assessment, *Tech. rep.*, Technical report, Riso National Laboratory, Denmark, 2012.

Bechmann, A. and Sørensen, N. N.: Hybrid RANS/LES method for wind flow over complex terrain, *Wind Energy: An International Journal for Progress and Applications in Wind Power Conversion Technology*, 13, 36–50, 2010.

Bechmann, A., Sørensen, N. N., Berg, J., Mann, J., and Réthoré, P.-E.: The Bolund experiment, part II: blind comparison of microscale flow 360 models, *Boundary-Layer Meteorology*, 141, 245, 2011.

Berg, J., Mann, J., Beechmann, A., Courtney, M., and Jørgensen, H. E.: The Bolund experiment, part I: flow over a steep, three-dimensional hill, *Boundary-layer meteorology*, 141, 219, 2011. and Kelly, M.: Atmospheric turbulence modelling, synthesis, and simulation, vol. 1, pp. 183–216, Institution of Engineering and Technology, [https://doi.org/10.1049/pbpo125f\\_ch5](https://doi.org/10.1049/pbpo125f_ch5), 2019.

Bhatnagar, P. L., Gross, E. P., and Krook, M.: A model for collision processes in gases. I. Small amplitude processes in charged and neutral 365 one-component systems, *Physical review*, 94, 511, 1954.

Blocken, B., Stathopoulos, T., and Carmeliet, J.: CFD simulation of the atmospheric boundary layer: wall function problems, *Atmospheric environment*, 41, 238–252, 2007.

Bowen, A. J. and Mortensen, N. G.: Exploring the limits of WAsP the wind atlas analysis and application program, in: *1996 European Wind Energy Conference and Exhibition*, HS Stephens & Associates, 1996.

370 Castro, F. A., Palma, J., and Lopes, A. S.: Simulation of the Askervein Flow. Part 1: Reynolds Averaged Navier–Stokes Equations (k epsilon Turbulence Model), *Boundary-Layer Meteorology*, 107, 501–530, 2003.

Chapman, S., Cowling, T. G., and Burnett, D.: The mathematical theory of non-uniform gases: an account of the kinetic theory of viscosity, thermal conduction and diffusion in gases, Cambridge university press, 1990.

Chen, S. and Doolen, G. D.: Lattice Boltzmann method for fluid flows, *Annual review of fluid mechanics*, 30, 329–364, 1998.

375 **Chen, X. P.: Applications of**

Davidson, P. A.: *Turbulence: an introduction for scientists and engineers*, Oxford University Press, 2015.

Deiterding, R. and Wood, S. L.: An adaptive lattice Boltzmann method to turbulent flow around two-dimensional airfoil, *Engineering Applications of Computational Fluid Mechanics* for predicting wake fields behind wind turbines, in: *New Results in Numerical and Experimental Fluid Mechanics X*, pp. 845–857, Springer, 2016.

380 DeLeon, R., Sandusky, M., and Senocak, I.: Simulations of turbulent flow over complex terrain using an immersed-boundary method, *Boundary-Layer Meteorology*, 167, 6, 572–580, 2012. 399–420, 2018.

d'Humieres, D.: Multiple-relaxation-time lattice Boltzmann models in three dimensions, *Philosophical Transactions of the Royal Society of London. Series A: Mathematical, Physical and Engineering Sciences*, 360, 437–451, 2002.

385 Dhunny, A., Lollchund, M., and Rughooputh, S.: Numerical analysis of wind flow patterns over complex hilly terrains: comparison between two commonly used CFD software, *International Journal of Global Energy Issues*, 39, 181–203, 2016.

Diebold, M., Higgins, C., Fang, J., Bechmann, A., and Parlange, M. B.: Flow over hills: a large-eddy simulation of the Bolund case, *Boundary-layer meteorology*, 148, 177–194, 2013.

Ferreira, A., Lopes, A., Viegas, D., and Sousa, A.: Experimental and numerical simulation of flow around two-dimensional hills, *Journal of wind engineering and industrial aerodynamics*, 54, 173–181, 1995.

390 Filippova, O., Succi, S., Mazzocco, F., Arrighetti, C., Bella, G., and Hänel, D.: Multiscale lattice Boltzmann schemes with turbulence modeling, *Journal of Computational Physics*, 170, 812–829, 2001.

Izham, M., Fukui, T., and Morinishi, K.: Application of regularized lattice Boltzmann method for incompressible flow simulation at high Reynolds number and flow with curved boundary, *Journal of Fluid Science and Technology*, 6, 812–822, 2011.

395 Kim, H. G., Patel, V., and Lee, C. M.: Numerical simulation of wind flow over hilly terrain, *Journal of wind engineering and industrial aerodynamics*, 87, 45–60, 2000.

Lange, J., Mann, J., Berg, J., Parvu, D., Kilpatrick, R., Costache, A., Chowdhury, J., Siddiqui, K., and Hangan, H.: For wind turbines in complex terrain, the devil is in the detail, *Environmental Research Letters*, 12, 094 020, 2017.

400 Latt, J.: Choice of units in lattice Boltzmann simulations, Freely available online at [http://lbmethod.org/\\_media/howtos:lbunits.pdf](http://lbmethod.org/_media/howtos:lbunits.pdf), 2008.

Latt, J. and Chopard, B.: Lattice Boltzmann method with regularized pre-collision distribution functions, *Mathematics and Computers in Simulation*, 72, 165–168, 2006.

Latt, J. et al.: Palabos, parallel lattice Boltzmann solver, *FlowKit*, Lausanne, Switzerland, 2009.

405 Ma, Y. and Liu, H.: Large-eddy simulations of atmospheric flows over complex terrain using the immersed-boundary method in the Weather Research and Forecasting Model, *Boundary-Layer Meteorology*, 165, 421–445, 2017.

Malaspinas, O., Chopard, B., and Latt, J.: General regularized boundary condition for multi-speed lattice Boltzmann models, *Computers & Fluids*, 49, 29–35, 2011.

Maurizi, A., Palma, J., and Castro, F.: Numerical simulation of the atmospheric flow in a mountainous region of the North of Portugal, *Journal of wind engineering and industrial aerodynamics*, 74, 219–228, 1998.

410 Onodera, N. and Idomura, Y.: Acceleration of wind simulation using locally mesh-refined lattice boltzmann method on gpu-rich supercomputers, in: *Asian Conference on Supercomputing Frontiers*, pp. 128–145, Springer, 2018.

Qian, Y.: D. d'Humi eres, and P. Lallemand, Lattice BGK models for Navier-Stokes equation, *Europhys. Lett*, 17, 479–484, 1992.

Schönherr, M., Kucher, K., Geier, M., Stiebler, M., Freudiger, S., and Krafczyk, M.: Multi-thread implementations of the lattice Boltzmann method on non-uniform grids for CPUs and GPUs, *Computers & Mathematics with Applications*, 61, 3730–3743, 2011.

Succi, S.: The lattice Boltzmann equation: for fluid dynamics and beyond, Oxford university press, 2001.

415 Wang, Y., MacCall, B. T., Hocut, C. M., Zeng, X., and Fernando, H. J.: Simulation of stratified flows over a ridge using a lattice Boltzmann model, *Environmental Fluid Mechanics*, pp. 1–23, 2018.

Zhang, C.: Numerical predictions of turbulent recirculating flows with a  $\kappa - \epsilon$  model, *Journal of Wind Engineering and Industrial Aerodynamics*, 51, 177–201, 1994.

**Table 3.** Computational Time. All Simulation were run on 80 cores (Intel Xeon E5-2630V4: 2.2 GHz)

Palabos		Fluent RANS	Fluent DES
Formulation	unsteady	steady	unsteady
Cell Count	41'585'372	10'055'540	10'055'540
Total CPU	40273.6	4821.8	58509.7
Time CPU	40'273.6	4'821.8	58'509.7
Time (s)			
	8.1	4.0	48.5
Seconds/(core			
—————million			
cells)			
SPCMC*			

\*Computational time per cpu core and million cells

**Nomenclatur**

**Quantitiy**

**Description**

**x**—Position in  
the east/west  
direction ()  
**y**—Position

in————— the  
north/south  
direction————()

**z**—Vertical  
position—————  
**s**—Total velocity

**θ**—u—East/west  
component of  
the velocity ()  
**v**—North/south  
component of  
the velocity

**θ**—w—Vertical  
component of  
the velocity

**θ**TKE  
Turbulent  
kinetic  
energy,  $\langle \theta \rangle$ ,  $\langle \theta^2 \rangle$

## Compare Results

Old File:

**wes-2019-106-manuscript-version1 (1).pdf**  
15 pages (2.77 MB)  
17/12/2019 23:17:01

versus

New File:

**wesc19\_complexterrain\_200514.pdf**  
17 pages (2.81 MB)  
14/05/2020 15:42:04

**Total Changes**

**370**

**Content**

80	Replacements
154	Insertions
101	Deletions

**Styling and Annotations**

10	Styling
25	Annotations

[Go to First Change \(page 1\)](#)

# Evaluation of the Lattice Boltzmann Method for wind modelling in complex terrain

Alain Schubiger<sup>1</sup>, Sarah Barber<sup>1</sup>, and Henrik Nordborg<sup>1</sup>

<sup>1</sup>University of Applied Sciences Rapperswil (HSR)

<sup>1</sup>Oberseestrasse 10, 8640 Rapperswil CH

**Correspondence:** A.Schubiger (alain.schubiger@hsr.ch)

**Abstract.** The worldwide expansion of wind energy is making the choice of potential wind farm locations more and more difficult. This results in an increased number of wind farms being located in complex terrain, which is characterised by flow separation, turbulence and high shear. Accurate modelling of these flow features is key for wind resource assessment in the planning phase, as the exact positioning of the wind turbines has a large effect on their energy production and lifetime. Wind modelling for wind resource assessments is usually carried out with the linear model Wind Atlas Analysis and Application Program (WAsP), unless the terrain is complex, in which case Reynolds-Averaged Navier-Stokes (RANS) solvers such as WindSim and ANSYS Fluent are usually applied. Recent research has shown the potential advantages of Large Eddy Simulations (LES) for modelling the atmospheric boundary layer and thermal effects; however, LES is far too computationally expensive to be applied outside the research environment. Another promising approach is the Lattice Boltzmann Method (LBM), a computational fluid technique based on the Boltzmann<sup>10</sup> transport equation. It is generally used to study complex phenomena such as turbulence, because it describes motion at the mesoscopic level in contrast to the macroscopic level of conventional Computational Fluid Dynamics (CFD) approaches, which solve the Navier-Stokes (N-S) equations. Other advantages of LBM include its efficiency, near ideal scalability on High Performance Computers (HPC) and its ability to easily automate the geometry, the mesh generation and the post-processing. However, LBM has been applied very little<sup>11</sup> to wind modelling in complex terrain for wind energy applications, mainly due to the lack of availability of easy-to-use tools as well as the lack of experience with this technique. In this paper, the capabilities of LBM to model wind flow around complex terrain are investigated using the Palabos framework and data from a measurement campaign from the Bolund Hill experiment in Denmark. Detached Eddy Simulations (DES) and LES in ANSYS Fluent are used as a numerical comparison. The results show that there is in general a good agreement between simulation and experimental data, and LBM performs better than RANS and DES. Some deviations<sup>12</sup> can be observed near the ground, close to the top of cliff and on the lee side of the hill. The computational costs of the three techniques are compared and it has been shown that LBM can perform up to five times faster than DES, even though the set-up was not optimised in this initial study. It can be summarised that LBM has a very high potential for modelling wind flow over complex terrain accurately and at relatively low costs, compared to solving the N-S conventionally. Further studies on other sites are ongoing.

25 1 Introduction

In order to assess the wind resource for both the planning and the assessment of wind farms, measurements and simulations of the prevailing wind conditions are required. Simulations are especially crucial in the observation of flows over complex terrain due to the large impact of steep inclines on the flow conditions. If the terrain shows only weak topographic changes or low hills, linear models can be used to make fast and sufficiently accurate yield forecasts (Berg and Kelly, 2019). The extremely low computational effort and ease of use makes such models the current industry standard. Due to their simplified formulation, however, such models fail in complex terrain and the predictions can be unreliable (Bowen and Mortensen, 1996). For complex flows, non-linear methods that solve the Navier-Stokes (N-S) equations are better suited. The successful use of Reynolds-Averaged Navier-Stokes (RANS) models has been demonstrated in many studies (e.g. Ferreira et al. (1995), Maurizi et al. (1998), Kim et al. (2000), Castro et al. (2003)), and they are being used increasingly in the industry. This is reflected by the recent development of wind energy specific tools using RANS-based Computational Fluid Dynamics (CFD), including WAsP-CFD (Bechmann, 2012) and WindSim (Dhunny et al., 2016). The RANS equations govern the transport of the averaged flow quantities, with the whole range of the scales of turbulence being modelled using turbulence closure schemes. The RANS-based modelling approach therefore greatly reduces the required computational effort and resources compared to fully-resolved methods, and is widely adopted for practical engineering applications. A more detailed modelling of turbulence is possible using Large Eddy Simulations (LES). LES lies between Direct Numerical Simulations (DNS) and turbulence closure schemes. The idea of this method is to compute the mean flow and the large vortices exactly. The small-scale structures are not simulated, but their influence on the rest of the flow field is parameterised by a heuristic model. However, the computational effort and the demands on the computational mesh increase drastically compared to RANS simulations, due to the need to resolve the small and important dynamic eddies in the boundary layer. Recent studies of the Bolund Hill blind test also show that it is still a great challenge to achieve sufficiently accurate predictions using LES simulations (Bechmann et al. (2011), Diebold et al. (2013), Ma and Liu (2017), DeLeon et al. (2018)). This is because, to accurately resolve the small-scale turbulent structures near walls at high Reynolds numbers, an extremely fine grid resolution is required.

The Detached Eddy Simulation (DES) method is a combination of LES and RANS. With this method, the flow is mostly calculated by LES, but the flow and vortices in wall regions are modelled by RANS. This method promises a strong reduction of the computational effort and the mesh requirements compared to LES. In addition, boundary layer modelling using RANS models makes it possible to use surface roughness models (Bechmann and Sørensen, 2010).

An alternative to solving the N-S equations with great potential is the Lattice Boltzmann Method (LBM). LBM has become more and more popular in recent years and is being continuously developed further. LBM has also been used successfully for initial studies in the field of wind energy. Most of these studies focus on the simulation of flows around wind turbines and wind farms or analyse the wake behaviour of turbines (e.g. Deiterding and Wood (2016), Asmuth et al. (2019)). Studies have shown that LBM is a valid alternative to conventional CFD methods and has many advantages (Wang et al., 2018). The main advantage of the method is its almost ideal scalability. This makes the application on High Performance Computers (HPC) attractive, but Graphics Processing Unit (GPU)-based LBM codes have also been implemented recently (Schönherr et al. (2011), Onodera

and Idomura (2018)). This makes it possible to perform computationally intensive LES simulations on a simple desktop in a reasonable time (Asmuth et al., 2019). However, LBM has not yet been assessed a great deal for the calculation of wind fields in complex terrain for wind energy applications.

The goal of this present paper is therefore to evaluate the capabilities of LBM for wind modelling in complex terrain. ANSYS Fluent is used as reference for comparisons, using both a RANS and a DES approach. The paper starts with a brief introduction of the theories behind LBM and the conventional N-S-based CFD calculations in Section 2, then introduces the simulation method applied in Section 3, discusses the results in Section 4, and finishes with the conclusions in Section 5.

## 2 Lattice Boltzmann Method theory

### 2.1 Numerical method and governing equations

Interest in LBM has been growing in the past decades as an efficient method for computing various fluid flows, ranging from low-Reynolds-number flows to highly turbulent flows (e.g. Chen and Doolen (1998), Filippova et al. (2001)). The first LBM models struggled with high-Reynolds-number flows due to numerical instabilities. To solve this problem, various adaptions such as regularised Finite Difference (Latt and Chopard, 2006), multiple relaxation time d'Humieres, 2002) or entropic methods (Ansumali and Karlin, 2000) have been developed.

LBM has the following advantages over N-S: 1. A linear equation with only local instability, making it more stable and perfectly scalable, 2. The dissipation is introduced locally by the collision term and does not depend on the lattice, and 3. the relaxation time includes both the regular viscous effects and its higher order modifications. A description of LBM can be found, for example in Chen and Doolen (1998). The governing equations describe the evolution of the probability density of finding a set of particles with a given microscopic velocity at a given location:

$$f_i(\mathbf{x} + \mathbf{c}_i \Delta t, t + \Delta t) = f_i(\mathbf{x}, t) + \Omega_i(\mathbf{x}, t) \quad (1)$$

for  $0 \leq i < q$ , where  $\mathbf{c}_i$  represents a discrete set of  $q$  velocities,  $f_i(\mathbf{x}, t)$  is the discrete single particle distribution function corresponding to  $c_i$  and  $\Omega_i$  an operator representing the internal collisions of pairs of particles. Macroscopic values such as density  $\rho$  and the flow velocity  $u$  can be deduced from the set of probability density functions  $f_i(\mathbf{x}, t)$ , such as:

$$\rho = \sum_{i=0}^{q-1} f_i, \quad \rho \mathbf{u} = \sum_{i=0}^{q-1} f_i \mathbf{c}_i \quad (2)$$

The set of allowed velocities in LBM is restricted by conservation of mass and momentum and by rotational symmetry (isotropy). Some of the most popular choices for the set of velocities are D2Q9 and D3Q27 lattices, referring to nine velocities in 2D and 27 velocities in 3D. For both of these lattices, the speed of sound in lattice units is given by  $c_s = 1/\sqrt{3}$  (Succi, 2001). The collision operator  $\Omega_i$  is typically modelled with the Bhatnagar–Gross–Krook (BGK) approximation (Bhatnagar et al., 1954). It assumes that the fluid locally relaxes to equilibrium over a characteristic, non-dimensional timescale  $\tau$ . The relaxation time  $\tau$  determines how fast the fluid approaches equilibrium and is thus directly dependent on the viscosity of

the fluid. The corresponding equilibrium probability density function  $f_i^{(eq)}$ , is defined as:

$$90 \quad \Omega_i = -\frac{1}{\tau} \left[ f_i(\mathbf{x}, t) - f_i^{(eq)}(\mathbf{x}, t) \right] \quad (3)$$

The equilibrium distribution function  $f_i^{(eq)}$  is a local function that only depends on density and velocity in the isothermal case. It can be computed thanks to a second order development of the Maxwell–Boltzmann equilibrium function (Qian, 1992):

$$95 \quad f_i^{(eq)} = w_i \rho \left[ 1 + \frac{\mathbf{c}_i \cdot \mathbf{u}}{c_s^2} + \left( \frac{\mathbf{c}_i \cdot \mathbf{u}}{2c_s} \right)^2 - \frac{\mathbf{u}^2}{2c_s^2} \right] \quad (4)$$

where  $w_i$  refers to the gaussian weights of the lattice. A Chapman–Enskog expansion, based on the assumption that  $f_i$  is given by the sum of the equilibrium distribution plus a small perturbation  $f_i^1$ :

$$99 \quad f_i = f_i^{(eq)} + f_i^{(1)}, \text{ with } f_i^{(1)} \ll f_i^{(eq)} \quad (5)$$

can be applied to equation 1 in order to recover the exact N-S equation for quasi-incompressible flows in the limit of long-wavelength (Chapman et al., 1990). The lattice pressure is thus given by  $p = c_s^2 \rho$  and the lattice viscosity is linked to the BGK relaxation parameter through:

$$100 \quad \nu = c_s^2 \left( \tau - \frac{1}{2} \right) \quad (6)$$

The numerical scheme is divided in two steps:

- A collision step where the BGK model is applied:

$$105 \quad f_i \left( \mathbf{x}, t + \frac{1}{2} \right) = f_i(\mathbf{x}, t) + \frac{1}{\tau} \left[ f_i^{(eq)}(\mathbf{x}, t) - f_i(\mathbf{x}, t) \right] \quad (7)$$

- A streaming step:

$$110 \quad f_i(\mathbf{x} + \mathbf{c}_i, t + 1) = f_i \left( \mathbf{x}, t + \frac{1}{2} \right). \quad (8)$$

In the collision step particle populations interact and change their velocity directions according to scattering rules. This operation is completely local which makes LBM well suited for parallelism. The streaming step consists of an advection of each discrete population to the neighbour node located in the direction of the corresponding discrete velocity. Since a boundary node has less neighbours than an internal node, some populations are missing at the boundary after each iteration. These populations need to be reconstructed, which is the purpose of the implementation of boundary conditions in LBM.

## 2.2 Turbulence modelling

Turbulence leads to the appearance of eddies with a wide range of length and time scales, which interact with each other in a dynamically complex way. Given the importance of the avoidance or promotion of turbulence in engineering applications, it is no surprise that a substantial amount of research effort is dedicated to the development of numerical methods to capture the important effects due to turbulence. The methods can be grouped into the following four categories:

- Turbulence models for Reynolds-Averaged Navier–Stokes (RANS) equations
- Large Eddy Simulation (LES)
- Detached Eddy Simulation (DES)
- Direct Numerical Simulation (DNS)

120 In this work, LES was applied for the LBM simulations. LES is an intermediate form of turbulence calculation which simulates the behaviour of the larger eddies. The method involves spacial filtering, which passes the larger eddies and rejects the smaller eddies. The effects on the resolved flow (mean flow plus large eddies) due to the smallest, unresolved eddies are included by means of a so-called sub-grid scale model. It is assumed that the sub-grid scales have the effect of a viscosity correction, which is proportional to the norm of the strain-rate tensor at the level of the filtered scales,  $\nu = \nu_0 + \nu_T$ .  $\nu_T$  is defined as:

$$\nu_T = (C\Delta)^2 |S| \quad (9)$$

where  $C$  is the Smagorinsky constant,  $\Delta$  is the grid size and the tensor-norm of the strain rate is defined as  $|S| = \sqrt{S : S}$ . The value of the Smagorinsky constant depends on the physics of the problem and usually varies between 0.1 and 0.2 far from boundaries (Davidson, 2015).

## 130 3 Simulations

### 3.1 The Bolund Hill Experiment

The Bolund field campaign took place from December 2008 to February 2009 on the Bolund Hill in Denmark. Bolund Hill is a 130 m long (east–west axis), 75 m wide (north–south axis) and 11.7 m high hill, situated near the Risø Campus of the Technical University of Denmark. Details of the experiment are described in Bechmann et al. (2011). The campaign showed 135 dominant wind directions from the west and south-west. Thus the wind has an extensive upwind fetch over the sea before encountering land, leading to a “steady” flow on the windward side of the hill. The wind first encounters a 10 m vertical cliff, after which air flows back down to sea level on the east side of the hill. A recirculation zone and a flow separation are expected due to this abrupt change of slope. During the campaign, 35 anemometers were deployed over the hill. The location of the measurement devices can be seen on Figure 1. Instrumentation included 23 sonic anemometers, 12 cup anemometers and two 140 lidars. At each measurement location, the three components of the wind velocity vector and their variances were recorded for four different dominant wind directions, three westerly winds originating from the sea ( $268^\circ$ ,  $254^\circ$  and  $242^\circ$ ) and one easterly wind originating from the land ( $95^\circ$ ). The mean wind speed during the measurements was around  $10 \text{ ms}^{-1}$ , leading to a Reynolds number of  $Re = uh/\nu \approx 10^7$  with the free stream velocity  $u = 10 \text{ ms}^{-1}$ , the hill height  $h$  and the kinematic viscosity  $\nu$ . The measured values are ten minute averages of measurements sampled at 20 Hz for sonic anemometers.

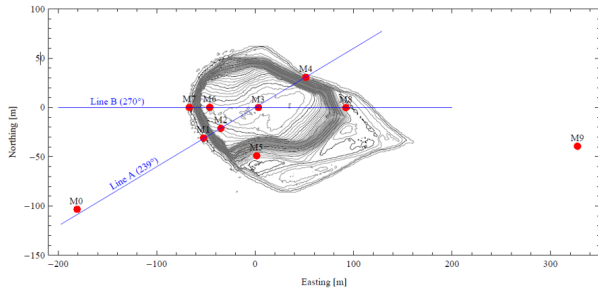


**Figure 1.** A contour map of Bolund Hill with meteorological masts denoted from M0 to M9.

145 **3.2 Simulations Set-Up**

**3.2.1 Boundary Conditions**

**Palabos**

The LBM flow solver used in this work was the Palabos open-source library (Latt et al., 2009). The Palabos library is a frame-

150 work for general-purpose CFD with a kernel based on LBM. The use of C++ code makes it easy for experienced programmers to install and run on any machine. It is thus possible for experienced modellers to set up fluid flow simulations with relative ease and to extend the open-source library with new methods and models, which is of paramount importance for the implementation of new boundary conditions.

To calculate the wind fields with Palabos in this work a 525 m long (east-west axis), 250 m wide (north-south axis) and 40 m high domain with a uniform grid resolution of  $\Delta x = \Delta y = \Delta z = 0.5$  m was used, leading to a total cell count of 46 million.

155 Palabos has the capability to include multiple grid sizes (octree grid structure) to refine the grid near the hill and coarsen it in the far-field, however these techniques were not in the scope of this first study. \*

There are no turbulence closure models or surface roughness models implemented in the Palabos library yet, therefore the water surfaces were prescribed as free-slip bounce back nodes and the ground surfaces were modelled using Regularised Bounce Back nodes (Malaspinas et al. (2011), Izham et al. (2011)). The bounce-back scheme in this first study was chosen 160 due to its simple implementation and robustness. There are more sophisticated models, like the Immersed Boundary Method, which may provide better accuracy than the staircase approximation of bounce-back nodes, which will be investigated in further studies.

The inlet profile was described according to the Bolund Hill Blind test specification for the westerly wind case. The logarithmic velocity profile is defined as:

165 
$$u(z_{agl}) \propto \frac{u_{*0}}{\kappa} \ln \left( \frac{z_{agl}}{z_0} \right) \quad (10)$$

\*with  $\kappa = 0.4$ , the friction velocity  $u_{*0} = 0.4$ , the elevation above ground level  $z_{agl} = z - gl$  ( $gl = 0.75$  m) and the roughness length  $z_0 = 0.0003$  m. Additionally, a time varying fluctuation of the wind speed, corresponding to the given turbulence inten-

sity value, was superposed. The logarithmic wind profile was updated every second during the simulation. The Atmospheric Boundary Layer (ABL) was considered neutral and thermal effects are therefore neglected. Both sides and top of the domain  
170 were modelled as free-slip walls (zero normal velocity). The outlet was set to a constant pressure. Each simulation was run for 600 s with a time step  $\Delta t = 2.89$  ms, leading to around 10 advection times. The relaxation time  $\tau$ , respectively the viscosity  $\nu$ , was chosen to respect eq. 6 and to stabilise the solution. The Smagorinsky constant was set to 0.14.

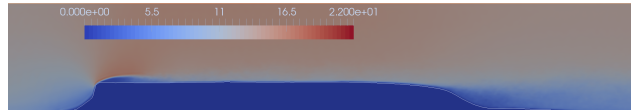
## Fluent

ANSYS Fluent contains the broad, physical modelling capabilities needed to model flow, turbulence, heat transfer and reactions  
175 for industrial applications, ranging from air flow over an aircraft wing to combustion in a furnace, from bubble columns to oil platforms, from blood flow to semiconductor manufacturing and from clean room design to wastewater treatment plants. For the Fluent simulations in this work the mesh was created with the new improved Fluent meshing tool, additionally the domain was extended to 830 m x 450 m x 60 m and two mesh refinement zones near the hill were implemented. The mesh resolution ranged from 0.5 m near the hill up to 15 m in the far-field, resulting in a total cell count of 10 million. A roughness length  
180 of  $z_0 = 0.3$  mm was prescribed for the water surface and a roughness length of  $z_0 = 15$  mm for the ground surfaces. The RANS simulation, using the  $k-\omega$  SST turbulence model, was used to initialise the flow and turbulence quantities for the DES simulation. Each simulation was run for 600 s with a time step  $\Delta t$  of 50 ms, leading to around seven advection times for the DES Fluent simulations. The inlet velocity was described as discussed before. According to the Blind Test, the turbulent kinetic energy (TKE) at the inlet was set to  $0.928 \text{ m}^2\text{s}^{-2}$ . For the DES model the Synthetic Turbulence Generator scheme  
185 was used to generate a time-dependent inlet condition. It uses a Fourier based synthetic turbulence generator. This method is inexpensive in terms of computational time compared with the other existing methods while achieving high quality turbulence fluctuations (ANSYS, 2019). Free-slip boundary condition is used for all the flow variables at the top and the side boundaries. The Smagorinsky constant was set to 0.14.

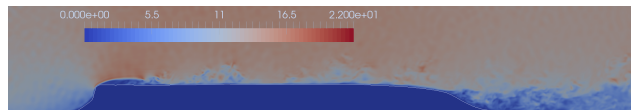
## 4 Results and Discussion

### 190 4.1 Flow comparisons

The calculated velocity magnitude fields at a vertical plane through the position of met mast M3 for each measurement technique are shown in Fig. 2 and Fig. 3. The LBM results are shown in Fig. 2, in terms of the averaged velocity magnitude over the simulation time (a) and the instantaneous velocity magnitude at time  $t = 600$  s (b). Fig. 3a and 3b show the averaged velocity magnitude over the simulation time for the RANS and DES simulations and Fig. 3c shows the instantaneous velocity magnitude at time  $t = 600$  s for DES. It is interesting to note the separation region as the wind flows over the sharp edge of the hill, as well as the highly separated flow at its rear side.



(a) Averaged velocity field.



(b) Instantaneous velocity field at  $t = 600$  s (LBM).

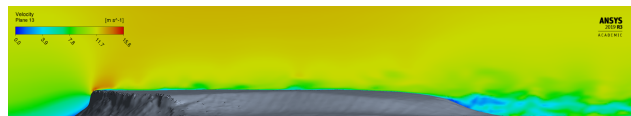
**Figure 2.** Velocity field over the hill along the B line (LBM)



(a) Averaged velocity field (RANS).



(b) Averaged velocity field (DES).



(c) Instantaneous velocity field (DES).

**Figure 3.** Velocity field over the hill along the B line (Fluent results)

## 4.2 Performance comparisons

For a quantitative comparison, the same methodology is used as described by Bechmann et al. (2011) for the wind flow along the 270° axis (Case 1) as shown in Fig. 1. This involved investigating the difference between measurements and simulations after 200 the mast M0 by comparing and quantifying the changes in the wind field as both changes in speed (so-called "speed-up") and in direction (so-called "turning"). Speed-up is defined as:

$$\Delta S_m = \frac{\langle \bar{s} \rangle_{z_{agl}} - \langle \bar{s}_0 \rangle_{z_{agl}}}{\langle \bar{s}_0 \rangle_{z_{agl}}} \quad (11)$$

📍📍📍📍📍📍📍📍 where  $\bar{s}$  is the mean wind speed at the sensor location and  $\bar{s}_0$  is the mean wind speed at the mast M0. Turning is defined as the difference between the wind direction at the measurement point and that at M0. The comparison is made in Fig. 5 for 205 two different elevations, 2 m and 5 m above the ground level and for the four masts along the B line (M7, M6, M3 and M8).

**Table 1.** Average Speed-up error

	Error at 2 m	Error at 5 m	Average error
Palabos LES	15.7	0.3	8.0
Fluent RANS	14.6	5.5	10.0
Fluent DES	27.4	7.1	17.3

The simulation results for the speed-up (Fig. 4) show good agreement with experimental data for all simulation techniques at 5 m above ground level (agl), with all deviations lower than 7.1% and the average speed-up error for each simulation technique shown in Table 1. The average speed-up error is defined as:

$$R_s = 100(\Delta S_s - \Delta S_m) \quad (12)$$

210 where  $S_m$  is the measured speed-up and  $S_s$  is the simulated speed-up defined by Eq. 11. Table 1 also allows the three simulation techniques to be compared to each other. The results 2 m agl show higher deviations in general, with the average speed-up error for each simulation technique shown in Table 1. The highest discrepancy can be seen at M6, which is probably due to the 215 separation bubble observed in the velocity fields in Fig. 2a. The experiment showed reduction in wind speed at M6, whereas the simulations all show an increase in wind speed. This leads to the conclusion that the actual separation bubble is larger than the simulated one. This could be due to an error in the CAD capture of the overhang of the hill noted in previous studies (Lange 220 et al., 2017). Furthermore, all the simulation techniques under-predicted the negative speed-up in the highly separated region of M8 compared to the experiment. The reason for this is probably due to the well-known difficulty of correctly simulating the separation point in CFD. As this effect is particularly pronounced at a height of 2 m above ground, it may be due to the fact that the lower measuring points lie within the boundary layer and the used models were not able to capture the near-wall flow 225 entirely correctly, perhaps due to the assumptions regarding surface roughness.

As shown in Table 1, the most accurate overall prediction was the LBM simulation, with an average error over all the 230 measurement positions of 8.0%. The RANS and DES mean errors are 10.0% and 17.3%, respectively. All three methods showed significantly more accurate results at 5 m than at 2 m above ground.

For the turning of the wind, a similar behaviour can be observed. The results match the experimental data very well at 5 m agl, with all deviations lower than 3.0% and the average turning error for each simulation technique shown in Table 2. As 225 for the speed-up, the deviations in turning are higher at 2 m agl, with the average turning error for each simulation technique shown in Table 2. The highest discrepancy can be seen at M8. Met mast M8 is located at the lee side in the recirculation zone of the hill. All the simulation results struggle to capture the flow accurately in terms of the turning. This could be due to the 230 inaccuracy in predicting the exact separation location on the rear of the hill, as mentioned above. Further analysis using the entire set of measurement data is shown in Fig. 7, in which a comparison between the simulation and experimental data for all three simulation methods is shown. Overall there is a good agreement between the measurements and simulated results.

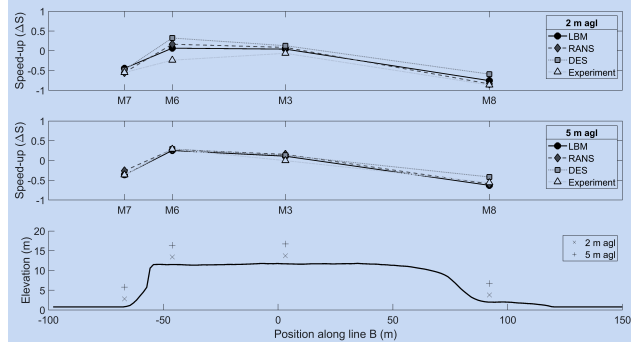


**Figure 4.** Speed-up along the Bolund Hill. Wind direction is from 270°

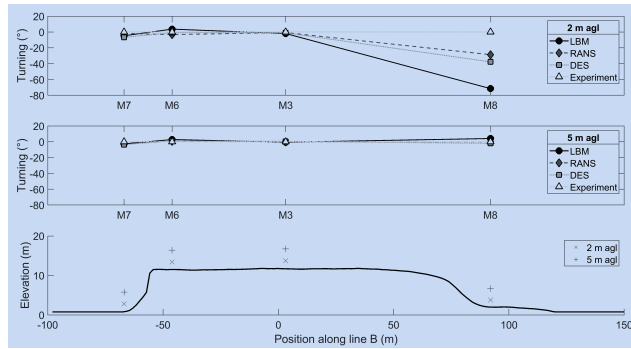


**Figure 5.** Turning along the Bolund Hill. Wind direction is from 270°

M2 and M6, both right after the edge of the cliff, show the biggest mismatch due to the detached flow after the edge of the hill, as discussed above. The next two figures show the ratio of simulated wind speeds to measured wind speeds as function of elevation (Fig. 8) and measurement location (Fig. 9). The biggest deviation between the data can again be seen at lower 235 heights and at mast M2, M6 and M8. Between the simulation methods, LBM shows the highest averaged deviation of the heights and at mast M2, M6 and M8. Between the simulation methods, LBM shows the highest averaged deviation of the ratios. The DES and RANS model perform both better in this comparison. This may be due to both these models use the  $k-\omega$  240 SST turbulence model and incorporate the surface roughness to calculate the near wall turbulence. The reason for the DES model performing worse than the RANS model is unclear at this point and requires further investigation.

Finally figure 6 shows the simulated turbulence kinetic energy (TKE) compared to the measurements for met masts M7, M6, 245 M3 and M8. Overall there is not a particularly good agreement between the measured and simulated data. All the simulations show similar but lower values for TKE. Especially at M6, at the cliff, the deviation is the highest. This discrepancy is being further investigated, but several authors have reported difficulties in simulating a horizontally homogeneous ABL flow in at least the upstream part of computational domains (Blocken et al. (2007), Zhang (1994)).

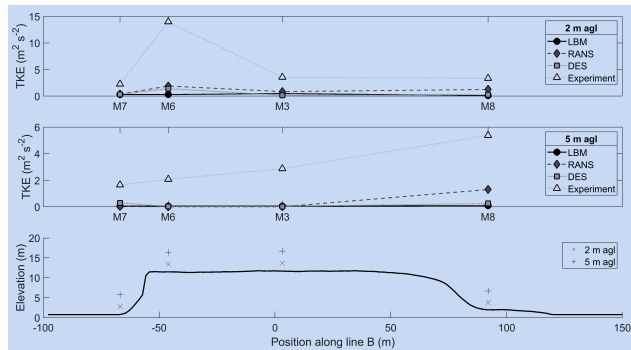


**Figure 6.** Turbulence kinetic energy along the Bolund Hill. Wind direction is from  $270^\circ$

**Table 2.** Average Turning error

	Error at 2 m	Error at 5 m	Average error
Palabos LES	-6.2	0.9	-2.7
Fluent RANS	3.0	0.4	0.2
Fluent DES	-2.7	1.7	-2.0

### 4.3 Cost comparisons

245 In this section, the performance of the simulation techniques is compared in terms of the computational costs. This has been done because the overall cost of a simulation is an important factor for modellers, who need to choose the most suitable model for a given wind energy project. The results of this work have been used in order to develop a new method for helping wind modellers choose the most cost-effective model for a given project. This was done by firstly defining various parameters for predicting the skill and cost scores before carrying out the simulations as well as for calculating skill and cost scores after 250 carrying out the simulations. Weightings were then defined for these parameters, and values assigned to them for a range of tools, including the ones applied in the present work, using a template containing pre-defined limits in a blind test. This allowed a graph of predicted skill score against cost score to be produced, enabling modellers to choose the most cost-effective model without having to carry out the simulations beforehand. More details can be found in Barber (2020).

Figure 10 and Table 3 summarise the computational costs for the three different techniques applied in this paper. It can clearly be seen that the LBM performed five times faster than the DES simulation and only slightly slower than the steady RANS simulation. This is due to its explicit formulation and exact advection operator. Furthermore, each of the collision and streaming processes are independent at each lattice, which makes the method so suitable for parallelisation. This advantage extends also to other types of high performance hardware like Graphics Processing Units (GPUs). Some studies of GPUs-based LBM solvers show promising results in this field (Asmuth et al. (2019), Schönher et al. (2011), Onodera and Idomura (2018)).

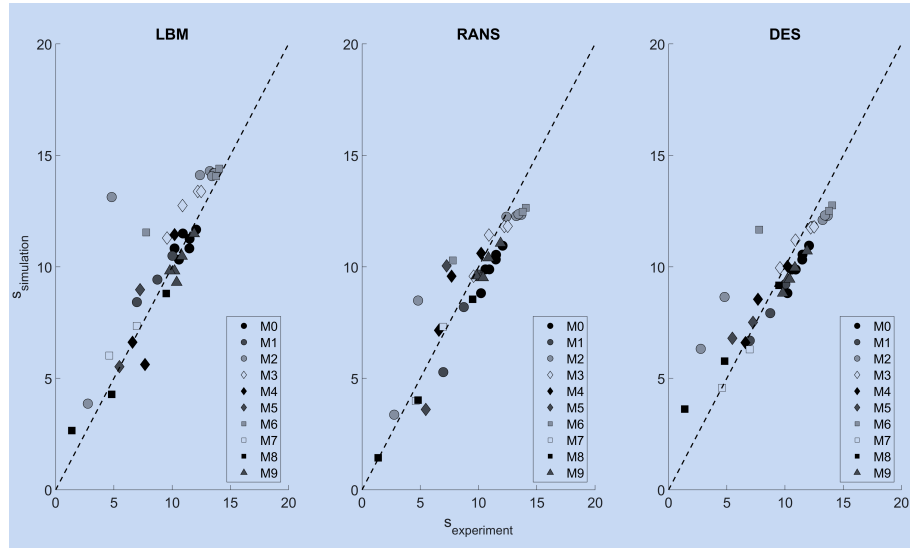


**Figure 7.** Scatter plot of wind speeds, measurement against simulation results

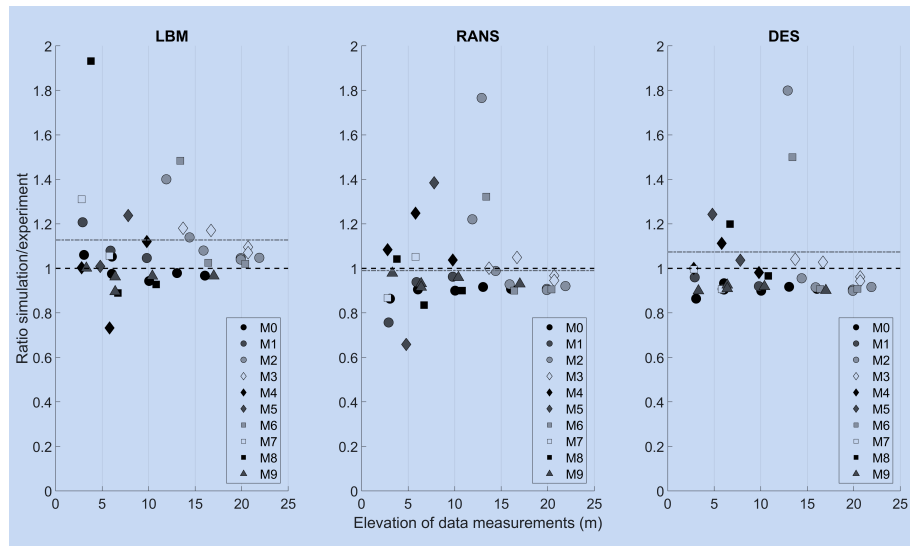


**Figure 8.** Ratio of simulation results to experimental wind speeds as function of elevation. The dotted grey line represents the average value.

260 The performance of this LBM simulation could be increased by adapting the code to use different grid sizes, depending on the flow and therefore reducing the overall cell count drastically. Incorporating the same grid refinement zones as used in the Fluent simulation, while maintaining the extended domain zone, the cell count for the resulting grid would decrease by a factor of five to seven. Work on this is ongoing.

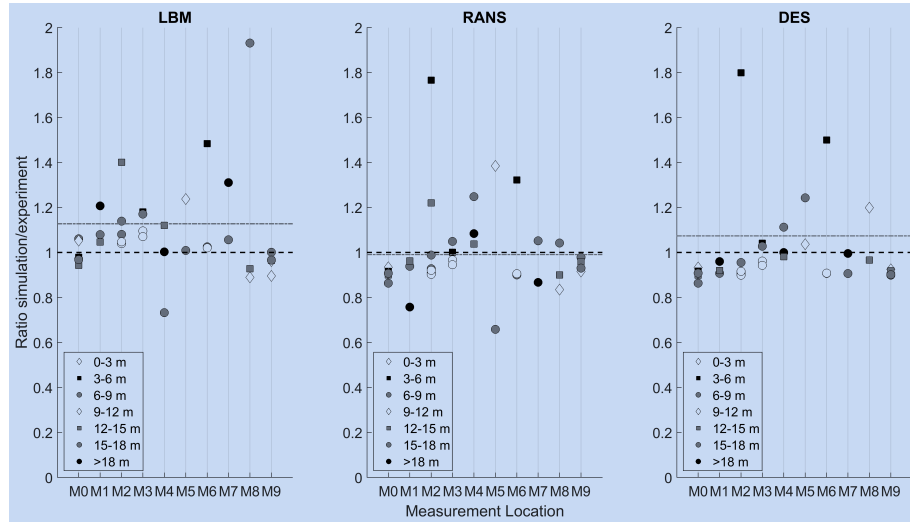


**Figure 9.** Ratio of simulation results to experimental wind speeds as function of measurement location. The dotted grey line represents the average value.



**Figure 10.** Comparison of computational time per cpu core and million cells

## 5 Conclusion

265 In this study, a LES simulation using the LBM framework Palabos was implemented to calculate the wind field over the complex terrain of the Bolund Hill. Advantages of LBM include its efficiency, near ideal scalability on High Performance Computers (HPC) and the capabilities to easily automate the geometry, the mesh generation and the post-processing.

The results were compared to RANS and DES simulations using ANSYS Fluent and field measurements. In general there was a good agreement between simulation and experimental data. The average wind speed-up error compared to measurements 270 was 8.0% for LBM, 17.3% for DES and 10.0% for RANS. The average wind turning error compared to measurements was

**Table 3.** Computational Time. All Simulation were run on 80 cores (Intel Xeon E5-2630V4: 2.2 GHz)

	Palabos	Fluent	Fluent DES
	RANS		
Formulation	unsteady	steady	unsteady
Cell Count	41'585'372	10'055'540	10'055'540
CPU Time (s)	40'273.6	4'821.8	58'509.7
SPCMC*	8.1	4.0	48.5

\*Computational time per cpu core and million cells

2.7° for LBM, 2.0° for DES and 0.2° for RANS. Some deviations could be observed near the ground, close to the top of the cliff (M2) and on the lee side of the hill (M8). Larger deviations could be observed for the TKE calculation, especially at met mast M6, which is positioned right after the edge of the cliff. This corresponds to previous work, which shows difficulties in correctly resolving the TKE.

275 The computational costs of these three models were compared and it has been shown that LBM, even in this not-yet fully optimised set-up of the simulation, can perform five times faster than DES and lead to slightly more accurate results.

It can be summarised that LBM may be applicable to modelling wind flow over complex terrain accurately at relatively low costs if the challenges raised in this work are addressed. Further studies on other sites are ongoing.

*Code availability.* [https://gitlab.com/aschubig/lbm\\_bollundhill.git](https://gitlab.com/aschubig/lbm_bollundhill.git)

## 280 Appendix A: Non-dimensioning procedure

The non-dimensioning procedure used in this study is done according to the similarity theory. It consists of two steps. First a physical system is converted into a dimensionless, independent of the original physical scales, but also independent of simulation parameters. In a second step, the dimensionless system is converted into a discrete simulation. Thus the dimensionless level (D) links the physical system (P) with the discrete Lattice-Boltzmann system (LB). The solutions to the incompressible

285 Navier-Stokes equations for example depend only on the Reynolds number (Re). Thus, the three systems are defined to have the same Reynolds number. The transition from (P) to (D) is made through the choice of a characteristic length scale  $l_0$  and time scale  $t_0$ , and the transition from (D) to (LB) through the choice of a discrete space step  $\Delta x$  and time step  $\Delta t_{\text{Latt}}$  (Latt, 2008).

*Author contributions.* The contribution of the authors in this paper is:

-  Alain Schubiger: carrying out and analysing the simulations.
-  Sarah Barber: project management and paper correction.
- Henrik Nordborg: supervision of Alain Schubiger and paper correction.

## References

Ansumali, S. and Karlin, I. V.: Stabilization of the lattice Boltzmann method by the H theorem: A numerical test, *Physical Review E*, 62, 295 7999, 2000.

ANSYS: Fluent Theory Guide, 2019.

Asmuth, H., Olivares-Espinosa, H., Nilsson, K., and Ivanell, S.: The Actuator Line Model in Lattice Boltzmann Frameworks: Numerical Sensitivity and Computational Performance, in: *Journal of Physics: Conference Series*, vol. 1256, p. 012022, IOP Publishing, 2019.

Barber, S.: Comparison metrics microscale simulation challenge for wind resource assessment – stage 1, 300 <https://doi.org/10.5281/zenodo.3743247>, <https://doi.org/10.5281/zenodo.3743247>, 2020.

Bechmann, A.: WAsP CFD A new beginning in wind resource assessment, Tech. rep., Technical report, Riso National Laboratory, Denmark, 2012.

Bechmann, A. and Sørensen, N. N.: Hybrid RANS/LES method for wind flow over complex terrain, *Wind Energy: An International Journal for Progress and Applications in Wind Power Conversion Technology*, 13, 36–50, 2010.

Bechmann, A., Sørensen, N. N., Berg, J., Mann, J., and Réthoré, P.-E.: The Bolund experiment, part II: blind comparison of microscale flow models, *Boundary-Layer Meteorology*, 141, 245, 2011.

Berg, J. and Kelly, M.: Atmospheric turbulence modelling, synthesis, and simulation, vol. 1, pp. 183–216, Institution of Engineering and Technology, [https://doi.org/10.1049/pbpo125f\\_ch5](https://doi.org/10.1049/pbpo125f_ch5), 2019.

Bhatnagar, P. L., Gross, E. P., and Krook, M.: A model for collision processes in gases. I. Small amplitude processes in charged and neutral one-component systems, *Physical review*, 94, 511, 1954.

Blocken, B., Stathopoulos, T., and Carmeliet, J.: CFD simulation of the atmospheric boundary layer: wall function problems, *Atmospheric environment*, 41, 238–252, 2007.

Bowen, A. J. and Mortensen, N. G.: Exploring the limits of WAsP the wind atlas analysis and application program, in: 1996 European Wind Energy Conference and Exhibition, HS Stephens & Associates, 1996.

Castro, F. A., Palma, J., and Lopes, A. S.: Simulation of the Askervein Flow. Part 1: Reynolds Averaged Navier–Stokes Equations (k epsilon Turbulence Model), *Boundary-Layer Meteorology*, 107, 501–530, 2003.

Chapman, S., Cowling, T. G., and Burnett, D.: The mathematical theory of non-uniform gases: an account of the kinetic theory of viscosity, thermal conduction and diffusion in gases, Cambridge university press, 1990.

Chen, S. and Doolen, G. D.: Lattice Boltzmann method for fluid flows, *Annual review of fluid mechanics*, 30, 329–364, 1998.

Davidson, P. A.: *Turbulence: an introduction for scientists and engineers*, Oxford University Press, 2015.

Deiterding, R. and Wood, S. L.: An adaptive lattice Boltzmann method for predicting wake fields behind wind turbines, in: *New Results in Numerical and Experimental Fluid Mechanics X*, pp. 845–857, Springer, 2016.

DeLeon, R., Sandusky, M., and Senocak, I.: Simulations of turbulent flow over complex terrain using an immersed-boundary method, *Boundary-Layer Meteorology*, 167, 399–420, 2018.

d'Humieres, D.: Multiple–relaxation–time lattice Boltzmann models in three dimensions, *Philosophical Transactions of the Royal Society of London. Series A: Mathematical, Physical and Engineering Sciences*, 360, 437–451, 2002.

Dhunny, A., Lollchund, M., and Rughooputh, S.: Numerical analysis of wind flow patterns over complex hilly terrains: comparison between two commonly used CFD software, *International Journal of Global Energy Issues*, 39, 181–203, 2016.

Diebold, M., Higgins, C., Fang, J., Bechmann, A., and Parlange, M. B.: Flow over hills: a large-eddy simulation of the Bolund case, 330 Boundary-layer meteorology, 148, 177–194, 2013.

Ferreira, A., Lopes, A., Viegas, D., and Sousa, A.: Experimental and numerical simulation of flow around two-dimensional hills, Journal of wind engineering and industrial aerodynamics, 54, 173–181, 1995.

Filippova, O., Succi, S., Mazzocco, F., Arrighetti, C., Bella, G., and Hänel, D.: Multiscale lattice Boltzmann schemes with turbulence modeling, Journal of Computational Physics, 170, 812–829, 2001.

Izham, M., Fukui, T., and Morinishi, K.: Application of regularized lattice Boltzmann method for incompressible flow simulation at high 335 Reynolds number and flow with curved boundary, Journal of Fluid Science and Technology, 6, 812–822, 2011.

Kim, H. G., Patel, V., and Lee, C. M.: Numerical simulation of wind flow over hilly terrain, Journal of wind engineering and industrial aerodynamics, 87, 45–60, 2000.

Lange, J., Mann, J., Berg, J., Parvu, D., Kilpatrick, R., Costache, A., Chowdhury, J., Siddiqui, K., and Hangan, H.: For wind turbines in 340 complex terrain, the devil is in the detail, Environmental Research Letters, 12, 094 020, 2017.

Latt, J.: Choice of units in lattice Boltzmann simulations, Freely available online at [http://lbmethod.org/\\_media/howtos:lbunits.pdf](http://lbmethod.org/_media/howtos:lbunits.pdf), 2008.

Latt, J. and Chopard, B.: Lattice Boltzmann method with regularized pre-collision distribution functions, Mathematics and Computers in Simulation, 72, 165–168, 2006.

Latt, J. et al.: Palabos, parallel lattice Boltzmann solver, FlowKit, Lausanne, Switzerland, 2009.

345 Ma, Y. and Liu, H.: Large-eddy simulations of atmospheric flows over complex terrain using the immersed-boundary method in the Weather Research and Forecasting Model, Boundary-Layer Meteorology, 165, 421–445, 2017.

Malaspinas, O., Chopard, B., and Latt, J.: General regularized boundary condition for multi-speed lattice Boltzmann models, Computers & Fluids, 49, 29–35, 2011.

Maurizi, A., Palma, J., and Castro, F.: Numerical simulation of the atmospheric flow in a mountainous region of the North of Portugal, 350 Journal of wind engineering and industrial aerodynamics, 74, 219–228, 1998.

Onodera, N. and Idomura, Y.: Acceleration of wind simulation using locally mesh-refined lattice boltzmann method on gpu-rich supercomputers, in: Asian Conference on Supercomputing Frontiers, pp. 128–145, Springer, 2018.

Qian, Y.: D. d'Humi eres, and P. Lallemand, Lattice BGK models for Navier-Stokes equation, Europhys. Lett, 17, 479–484, 1992.

Schönherr, M., Kucher, K., Geier, M., Stiebler, M., Freudiger, S., and Krafczyk, M.: Multi-thread implementations of the lattice Boltzmann 355 method on non-uniform grids for CPUs and GPUs, Computers & Mathematics with Applications, 61, 3730–3743, 2011.

Succi, S.: The lattice Boltzmann equation: for fluid dynamics and beyond, Oxford university press, 2001.

Wang, Y., MacCall, B. T., Hocut, C. M., Zeng, X., and Fernando, H. J.: Simulation of stratified flows over a ridge using a lattice Boltzmann model, Environmental Fluid Mechanics, pp. 1–23, 2018.

Zhang, C.: Numerical predictions of turbulent recirculating flows with a  $\kappa - \epsilon$  model, Journal of Wind Engineering and Industrial Aerodynamics, 360 51, 177–201, 1994.